NASA CR 132889

SOUTHEASTERN MASSACHUSETTS UNIVERSITY

SOUTHEASTERN MASSACHUSETTS UNIVERSITY · UNITATE · 1895 · FORTIOR

S M U
RESEARCH FOUNDATION

NORTH DARTMOUTH, MASS. 02747

Technical Report EE-73-6
Grant NASA/GSFC NGR 22-031-002
October 2, 1973

NONLINEAR ANALYSIS OF PHASE-LOCKED LOOPS WITH RAPIDLY VARYING PHASE

by

CHI-HAU CHEN, Senior Member, IEEE
and
MAISIE FAN, Student Member, IEEE
Southeastern Massachusetts University
North Dartmouth, Massachusetts 02747

Abstract

The performance of command and telemetry systems, useful in deep-space communications, is frequently affected by the radio-frequency phase error which is introduced at the point of reception by means of the carrier tracking loop. In low data rate communications, this phase error which is highly unpredictable may vary rapidly over the duration of the signaling interval. In this paper such phase variation is characterized by a sinusoidal input phase, $k \sin(\omega_0 t + \pi/6)$, which models a typical phase variation in communication over turbulent media. Conditions for synchronization stability and the acquisition behavior are examined by detailed computer study of the phase-plane trajectories for the second and third-order loops with perfect integrator. For k = 0.001, it is determined that $f_0/AK \leq 1/4$ for system stability. Here AK is the loop gain. For given f_0, the condition for stability is $kf_0 \leq 4$, except for very small f_0. Thus the loop is still useful under most fading conditions in deep space missions.

It is demonstrated that for the phase variation considered the third-order loop has no real advantage over the second-order loop. Finally, it is shown that nonzero initial conditions may result in large steady-state phase error.

Nonlinear Analysis of Phase-Locked Loops With Rapidly Varying Phase

C.H. Chen and M. Fan

I. Introduction

The performance of command and telemetry systems, useful in deep-space communications, is frequently affected by the radio-frequency phase error which is introduced at the point of reception by means of the carrier tracking loop. In low data rate communications, this phase error may vary rapidly over the duration of the signaling interval. Causes of this type of behavior in planetary entry are turbulence, dispersion, attenuation and residual doppler. The phase variations cannot be tracked by a phase-locked loop of lower bandwidth, while the signal-to-noise ratio in this minimum loop bandwidth is too low.

When the ratio of the system data rate to carrier tracking loop bandwidth is less than one, the problem of power allocation between the carrier and the data has been considered by Hayes and Lindsey [1] , Thomas [2], Sergo and Hayes [3]. For channels with time-varying phase, Heller [4] examined the performance of a sequential decoding system. An excellent treatment of the nonlinear analysis of the phase-locked loops is given by Viterbi [5] and Lindsey [6].

In this paper the phase variation is characterized by a sinusoidal input phase, $k \sin(\omega_0 t + \pi/6)$, which models a typical phase variation in communication over turbulent media. Nonlinear analysis of the loop in the absence of noise is performed by extensive computer study of the phase-plane trajectories. Conditions for synchronization stability and the acquisition behvaior can be examined from the phase-plane analysis. Both the second-order loop and the third-order loop with perfect integrators are considered with zero as well as nonzero initial conditions. Comparison is also made between the second-and the third-order loops with rapidly varying phase. Some preliminary computer results were reported by Chen [7] and Fan [8].

II. The Loop Equations

Following the notations of Viterbi ([5], Chapter 3), we consider first the differential equation of a second-order loop with perfect integrator.

$$\frac{d^2\phi}{dt^2} + AK\cos\phi\,\frac{d\phi}{dt} + aAK\sin\phi = \frac{d^2\theta_1}{dt^2} \tag{1}$$

where $\phi(t)$ is the phase error, AK is the loop gain, $\theta_1(t)$ is the phase of the input signal, and the transfer function of the loop filter is

$$F(s) = 1 + \frac{a}{s} \tag{2}$$

The loop can track the frequency ramp with zero steady state error. Now we consider the important case that $\theta_1(t)$ is varying several cycles over a bit interval of, say, 1 second which is typical in low data rate communications. The variation is normally caused by the time-varying channel. Let

$$\theta_1(t) = k\sin(\omega_0 t + \frac{\pi}{6}) \tag{3}$$

By normalizing the variables with

$$a' = \frac{a}{AK}\,,\ \tau = AKt,\ \phi' = \frac{d\phi}{d\tau}\,,\ \phi'' = \frac{d^2\phi}{d\tau^2} \tag{4}$$

Eq. (1) becomes

$$\ddot{\phi} + \dot{\phi}\cos\phi + a'\sin\phi = -\frac{k\omega_0^2}{(AK)^2}\sin\left(\frac{\omega_0\tau}{AK} + \frac{\pi}{6}\right) \tag{5}$$

which in turn can be written in the state equation form as

$$\begin{aligned}\dot{x}_1 &= x_2\\ \dot{x}_2 &= -x_2\cos x_1 - a'\sin x_1 - \frac{k\omega_0^2}{(AK)^2}\sin\left(\frac{\omega_0\tau}{AK} + \frac{\pi}{6}\right)\end{aligned} \tag{6}$$

where $x_1 = \phi(t)$. It is noted from Eq. (5) that the larger the loop gain, or the loop bandwidth, the smaller the frequency of the forcing function given by Eq. (3). The frequency f_o is reduced by a factor of AK, and the amplitude $k\omega_o^2$ is reduced by $(AK)^2$. In other words, the large loop gain reduces the effect of the time varying input phase $\phi_1(t)$.

For a third order loop with loop-filter transfer function

$$F(s) = 1 + \frac{a}{s} + \frac{b}{s^2} \tag{7}$$

the differential equation (Viterbi [5], p. 64) is

$$\frac{d^2\phi}{dt^2} + (AK\frac{d}{dt} + aAK)\sin\phi(t) + bAK\int_0^t \sin\phi(u)du = \frac{d^2\theta_1}{dt^2} \tag{8}$$

which, using Eqs. (4) and (3), can be reduced to

$$\ddot{\phi} + \dot{\phi}\cos\phi + a'\sin\phi + b'\int \sin\phi\, d\tau = -\frac{k\omega_o^2}{(AK)^2}\sin\left(\frac{\omega_o\tau}{AK} + \frac{\pi}{6}\right) \tag{9}$$

which in the state equation form becomes

$$\dot{x}_1 = x_2$$
$$\dot{x}_2 = -x_2\cos x_1 - a'\sin x_1 - b'\int \sin x_1\, d\tau - \frac{k\omega_o^2}{(AK)^2}\sin\left(\frac{\omega_o\tau}{AK} + \frac{\pi}{6}\right) \tag{10}$$

where

$$b' = \frac{b}{(AK)^2} \text{ and } x_1 = \phi(t).$$

Phase-plane analysis of Eqs. (6) and (10) is performed by using the second-order Runge-Kutta method (see, e.g. [9]). The computer results are reported in the following sections.

III. Nonlinear Analysis of the Second-Order Loop

Consider first $k = 0.001$. The loop behavior depends on the ratio f_o/AK. Let $a' = 1/2$ and $AK = 32$, the phase-plane plots of the loop are shown in Figs. 1(a), (b) and (c) with $f_o = 6.4$, 8.0 and 16.0 respectively. $f_o = 8.0$ appears to be the threshold value above which the loop would not be able to track the input phase. For $f_o/AK \leq 1/4$ the loop would settle with a stable "limit cycle." It is noted that the steady state error cannot be reduced to zero because of the continuous input phase variation. Thus $f_o/Ak \leq 1/4$ is the condition for stability. By increasing the number of points to 3000, Fig. 1(d) shows that the steady state trajectory drifts only slowly. The loop reaches the stable trajectory after less than two cycles of change in phase.

Next we examine the threshold value of k for specified f_o. Figs. 2,3,4,5,6 are the phase-plane plots for $f_o = 1.1$, 1.0, 0.8, 0.5, 0.25 respectively. The threshold here is not a critical value but it may be concluded that $kf_o \leq 4$ is the required condition for stability with AK = 16, a = 8. When f_o becomes small the allowable product kf_o rises rapidly. In the limit $f_o = 0$, kf_o can be any positive value. If the phase error varies one full cycle in one second, the above condition states that the maximum allowable phase error is 4 radians. This indicates that the loop can function properly under most fading conditions in deep space missions.

For example, based on the updated knowledge of the effect of turbulence in the Venus atmosphere on radio propagation [10], we anticipate that the phase-locked loop with proper bandwidth can maintain a continuous communication between the atmospheric probe and the Earth.

IV. Nonlinear Analysis of the Third-Order Loop

Consider the case k = 0.001, AK = 16, a = 8, b' = 1/32. Figs. 7(a), (b), (c) are the phase-plane plots of $\dot{\phi}$ vs ϕ for f_o = 3.2, 4.0 and [illegible].0 respectively. For the same ratios of f_o/AK, the trajectories of the third-order loop drift faster. $f_o/AK \leq 1/4$ also appears to be the threshold condition for stability. The increase of b' to b' = 1/16 as shown in Figs. 8(a), (b), (c) only causes the trajectories to drift more. The effect of increasing k is clearly illustrated in Figs. 9(a)-(d). The threshold value for k is in the region $0.1 < k < 1.0$. The condition for stability is $kf_o < 4$ which is consistent with the second-order loop results. A careful comparison is made between the second-order and the third-order loops by using exactly the same loop parameters AK = 8, a = 4, k = 0.001, f_o = 1.0 with printout of 1000 points. Both loops are stable and take the same amount of time (50 seconds) to cover 6 cycles of trajectories. The results are shown in Fig. 10(a) for the second-order loop and Figs. 10(b) and (c) for the third-order loop with b' = 1/32 and 1/8 respectively. It is noted that the third-order loop has larger phase error which increases with b'. Based on the above study, we may conclude that for the sinusoidal phase variation considered in this paper, the third-order loop has no real advantage over the second-order loop.

V. Effects of Nonzero Initial Conditions

To study the loop behaviors under different initial conditions, we consider both the second-order and third-order loops with AK = 8, a = 4, k = 0.001 for the initial conditions $(\dot{\phi}, \phi) = (-3.14, 6), (-3.14, 4), (-3.14, 2), (-3.14, 0)$. The results are shown in Fig. 11 for the second-order and Fig. 12 for the third-order loops with b' = 1/32. The trajectories in the lower half plane are the mirror image of those in the upper half plane with respect to the $\dot{\phi} = 0$ axis. It is interesting to note that, in all initial conditions considered, the loops reach a steady-state of $\dot{\phi} = 0$ and ϕ = constant in spite of the sinusoidal input phase. The steady-state phase errors may be too large, however, from practical viewpoint. Thus the nonzero initial conditions should be avoided if the large steady-state phase error is not tolerable.

VI. Concluding Remarks

We have examined the critical parameter values of the second and the third-order loops with rapidly varying phase which is modelled by a sinusoidal input phase variation. The nonlinear analysis is performed by studying the phase-plane trajectories. Although the third-order loop does not have the advantages as it normally has in tracking phase errors, some modification of the loop structure appears necessary to obtain a more efficient tracking system. Methods of signal acquisition aids, as suggested by Lindsey [6], especially the computer-aided acquisition for low signal-to-noise ratios should also be examined.

References

1. J.F. Hayes and W.C. Lindsey, "Power allocation - Rapidly varying phase error", IEEE Trans. on Communication Technology, pp. 323-326, April 1969.

2. C.M. Thomas, "Carrier reference power allocation for PSK at low data rates", International Communications Conference, June 1970.

3. J.R. Sergo, Jr. and J.F. Hayes, "Power allocation in a two way coherent communication systems", UMR - M.J. Kelly Communications Conference, paper no. 22-2-1, Rolla, Mo., October 1970.

4. J.A. Heller, "Sequential decoding for channels with time-varying phase", Ph.D. thesis, M.I.T., Cambridge, Mass. September 1967.

5. A.J. Viterbi, "Principles of Coherent Communication", McGraw-Hill Book Co., 1966.

6. W.C. Lindsey, "Synchronization Systems in Communication and Control", Prentice-Hall, Inc., 1972.

7. C.H. Chen, "Phase-plane analysis of phase-locked loops with rapidly varying phase", TR EE-73-4, SMU, N. Dartmouth, Mass., July 1973.

8. M. Fan, "Computer study of phase-locked loop behaviors with rapidly varying phase error", TR EE-73-5, SMU, N. Dartmouth, Mass., September 1973.

9. D.D. McCracken and W.S. Dorn, "Numerical Methods and Fortran Programming", Wiley, New York 1964.

10. J.W. Strohbehn, "The effect of turb ulence in the Venus atmosphere on radio propagation", paper preprint, August 1973, to be published.

S.M.U. SYSTEM SUBROUTINE - PLOTIT

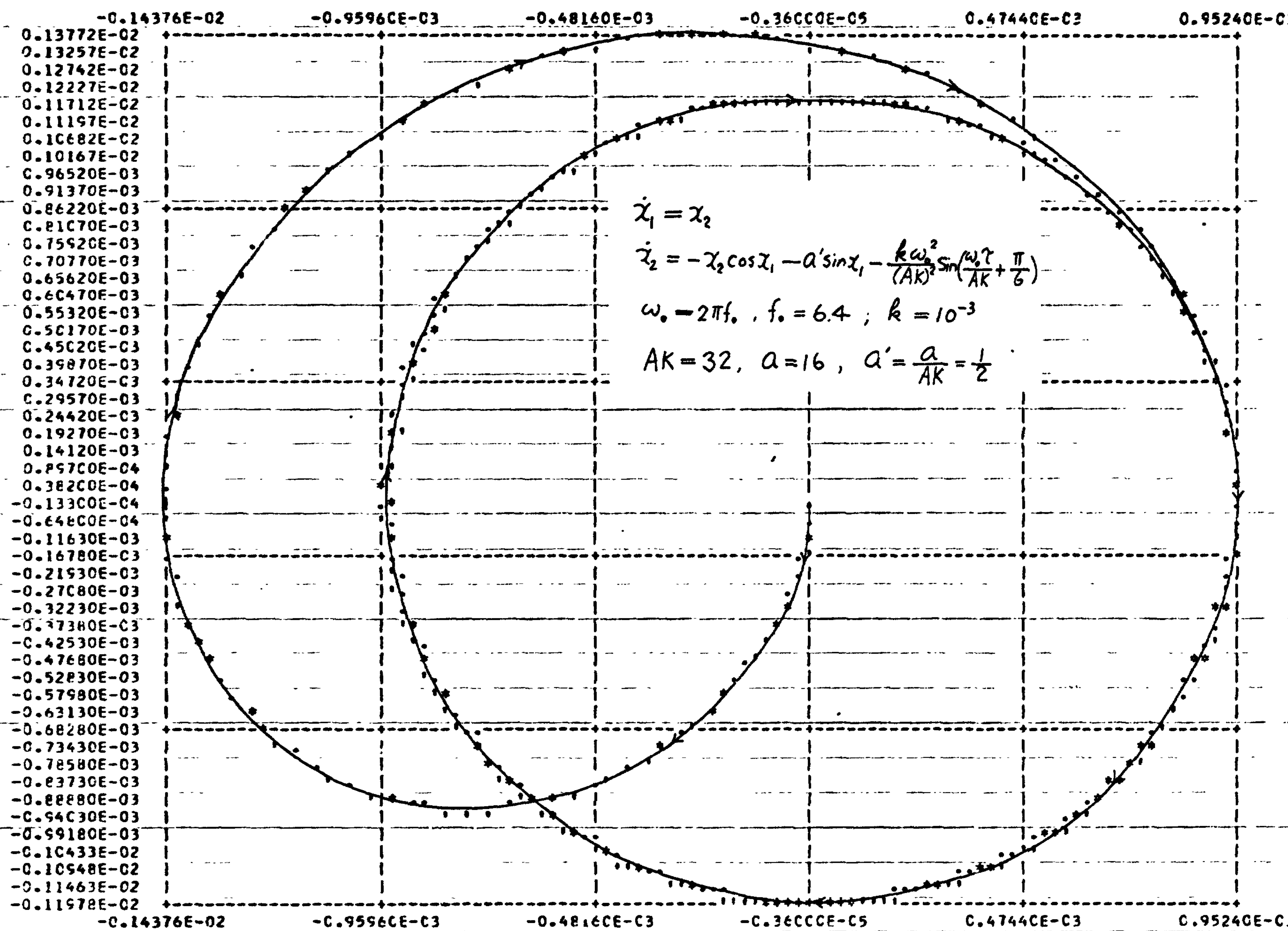

Fig. 1 (a)

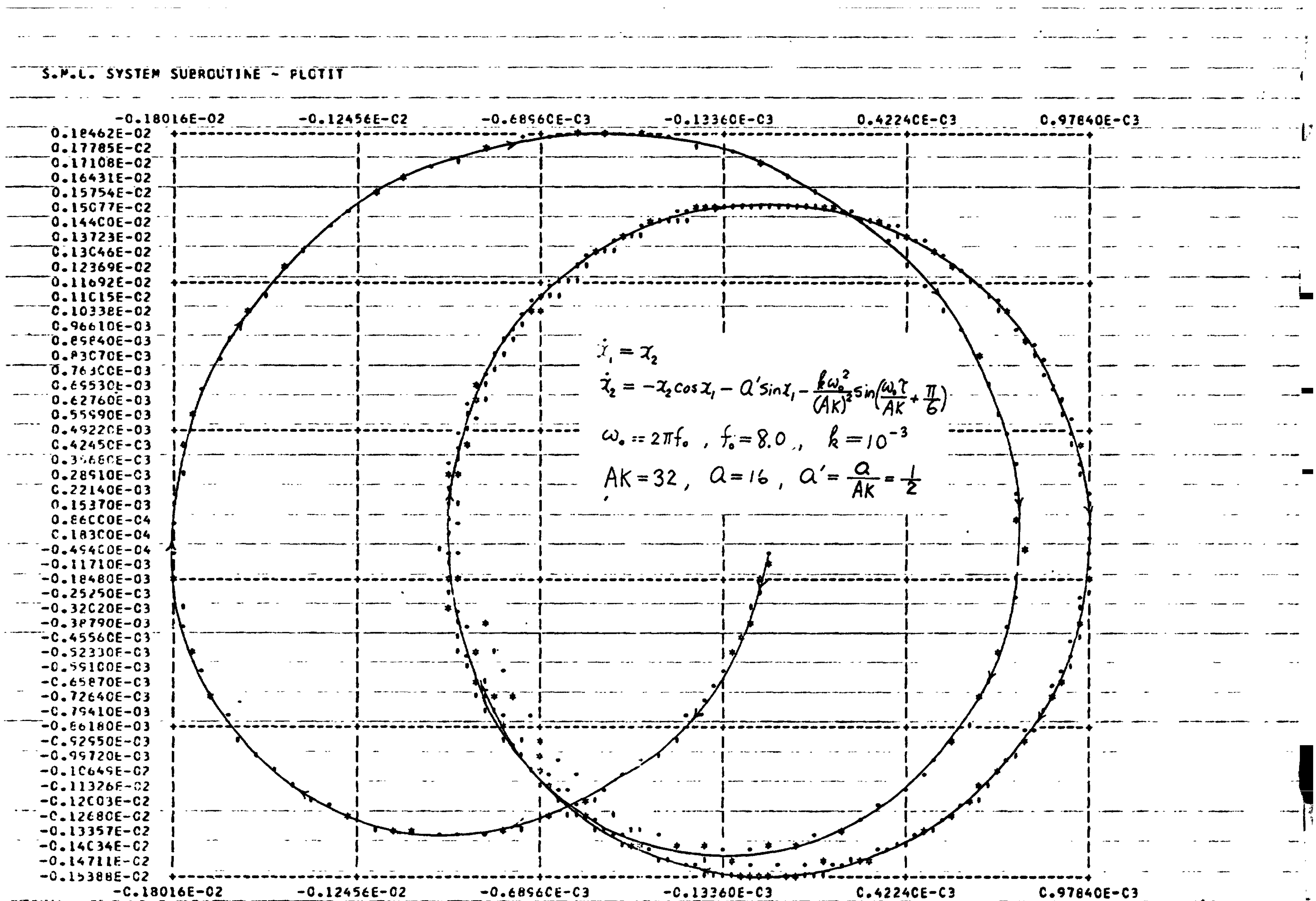
S.P.L. SYSTEM SUBROUTINE - PLOTIT
-0.18016E-02
-0.12456E-02
-0.6896CE-03
-0.13360E-03
0.4224CE-03
0.97840E-03
0.18462E-02
0.17785E-02
0.17108E-02
0.16431E-02
0.15754E-02
0.15077E-02
0.14400E-02
0.13723E-02
0.13046E-02
0.12369E-02
0.11692E-02
0.11015E-02
0.10338E-02
0.96610E-03
0.89840E-03
0.83070E-03
0.76300E-03
0.69530E-03
0.62760E-03
0.55990E-03
0.49220E-03
0.42450E-03
0.28910E-03
0.22140E-03
0.15370E-03
0.86CC0E-04
0.18300E-04
-0.49400E-04
-0.11710E-03
-0.18480E-03
-0.25250E-03
-0.32020E-03
-0.38790E-03
-0.45560E-03
-0.52330E-03
-0.59100E-03
-0.65870E-03
-0.72640E-03
-0.79410E-03
-0.86180E-03
-0.92950E-03
-0.99720E-03
-0.10649E-02
-0.11326E-02
-0.12003E-02
-0.12680E-02
-0.13357E-02
-0.14034E-02
-0.14711E-02
-0.15388E-02
$\dot{x}_1 = x_2$
$\dot{x}_2 = -x_2 \cos x_1 - a' \sin x_1 - \frac{k\omega_0^2}{(AK)^2} \sin\left(\frac{\omega_0 \tau}{AK} + \frac{\pi}{6}\right)$
$\omega_0 = 2\pi f_0$, $f_0 = 8.0$, $k = 10^{-3}$
$AK = 32$, $a = 16$, $a' = \frac{a}{AK} = \frac{1}{2}$

Fig. 1(b)

S.M.U. SYSTEM SUBROUTINE - PLOTIT

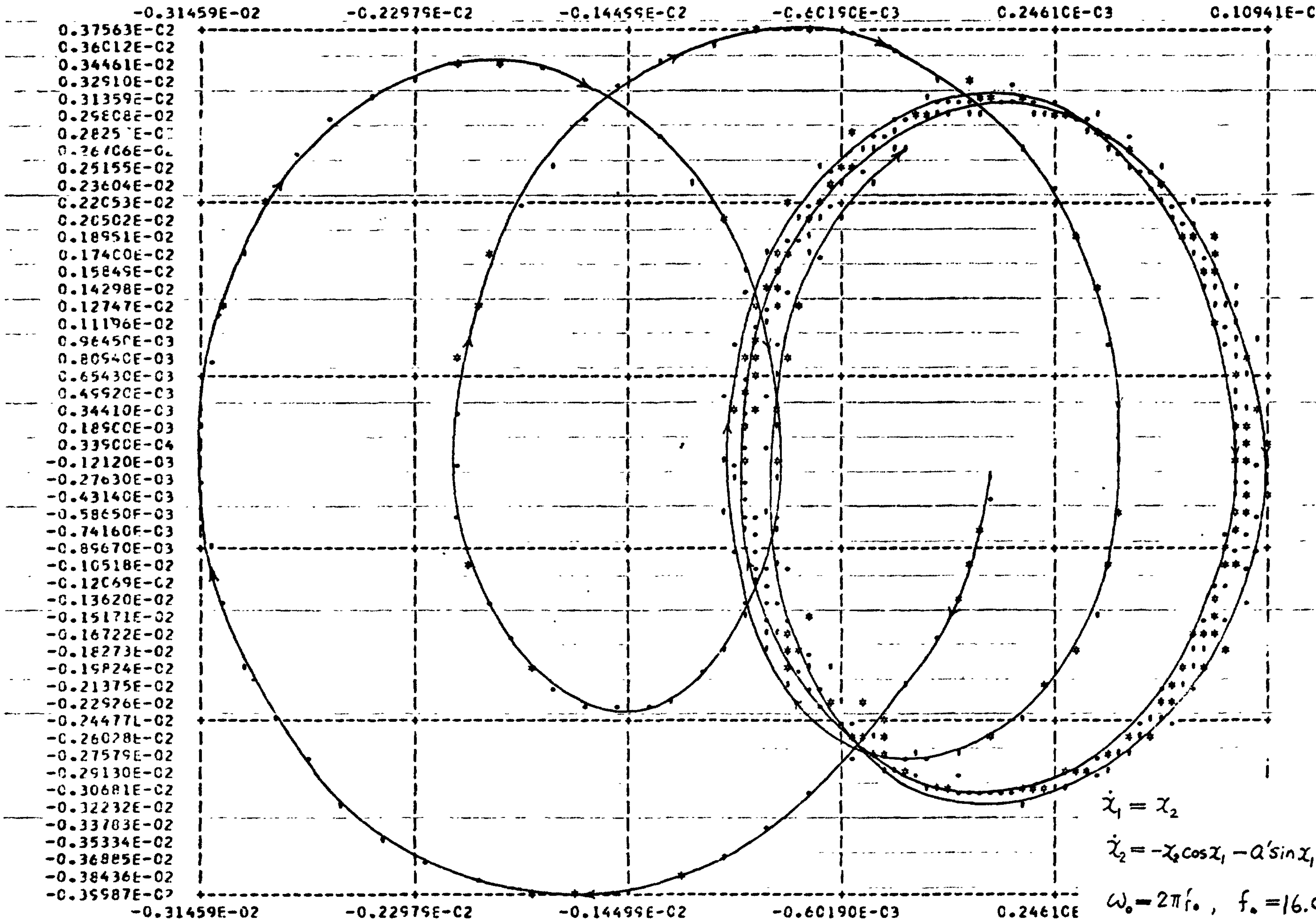

$\dot{x}_1 = x_2$

$\dot{x}_2 = -x_2\cos x_1 - a'\sin x_1 - \frac{k\omega_0^2}{(AK)^2}\sin\left(\frac{\omega_0\tau}{AK} + \frac{\pi}{6}\right)$

$\omega_0 = 2\pi f_0$, $f_0 = 16.0$, $k = 10^{-3}$

$AK = 32$, $a = 16$, $a' = \frac{a}{AK} = \frac{1}{2}$

Fig. 1(c)

S.P.C. SYSTEM SUBROUTINE - PLOTIT

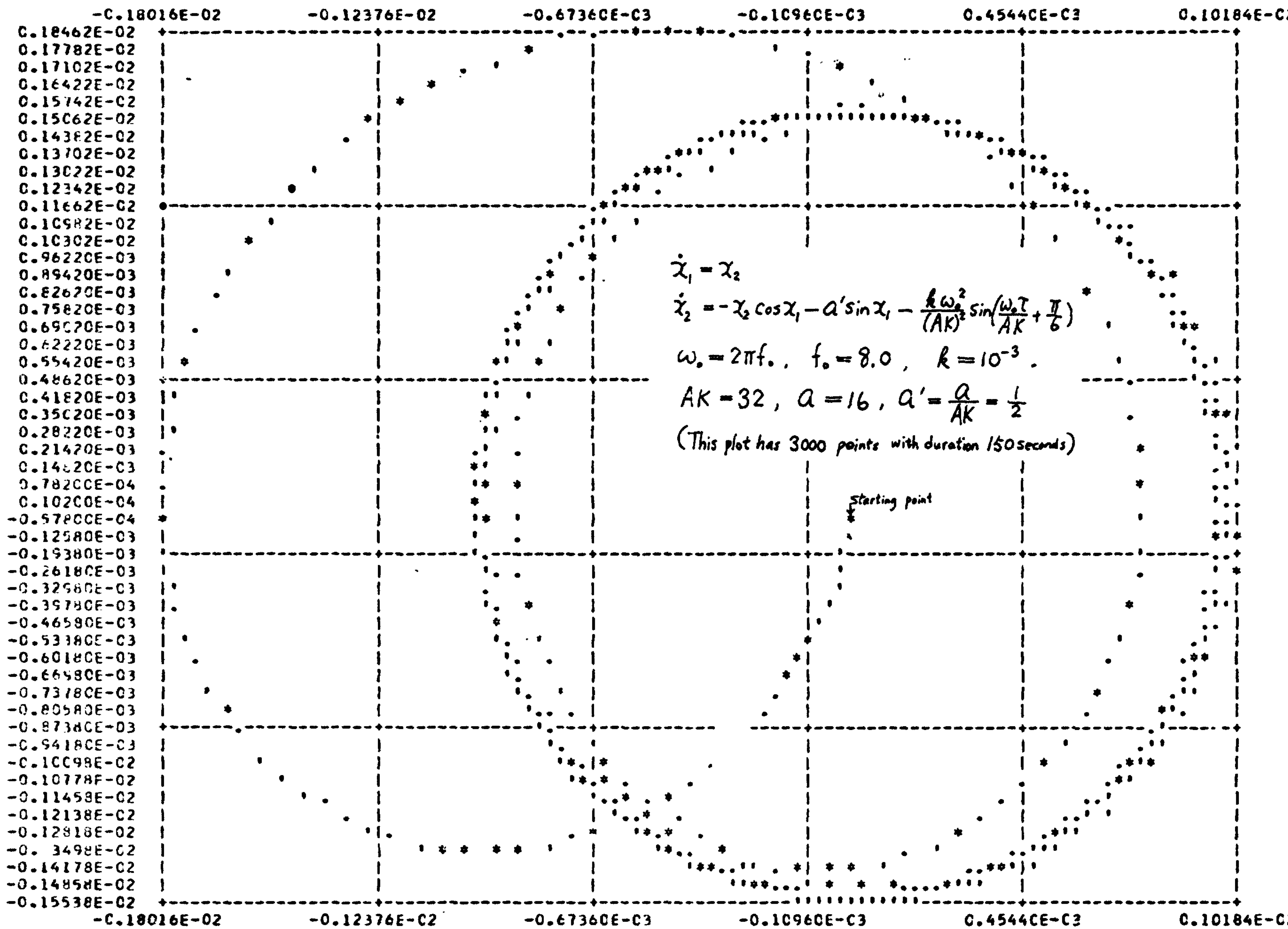

Fig. 1(d)

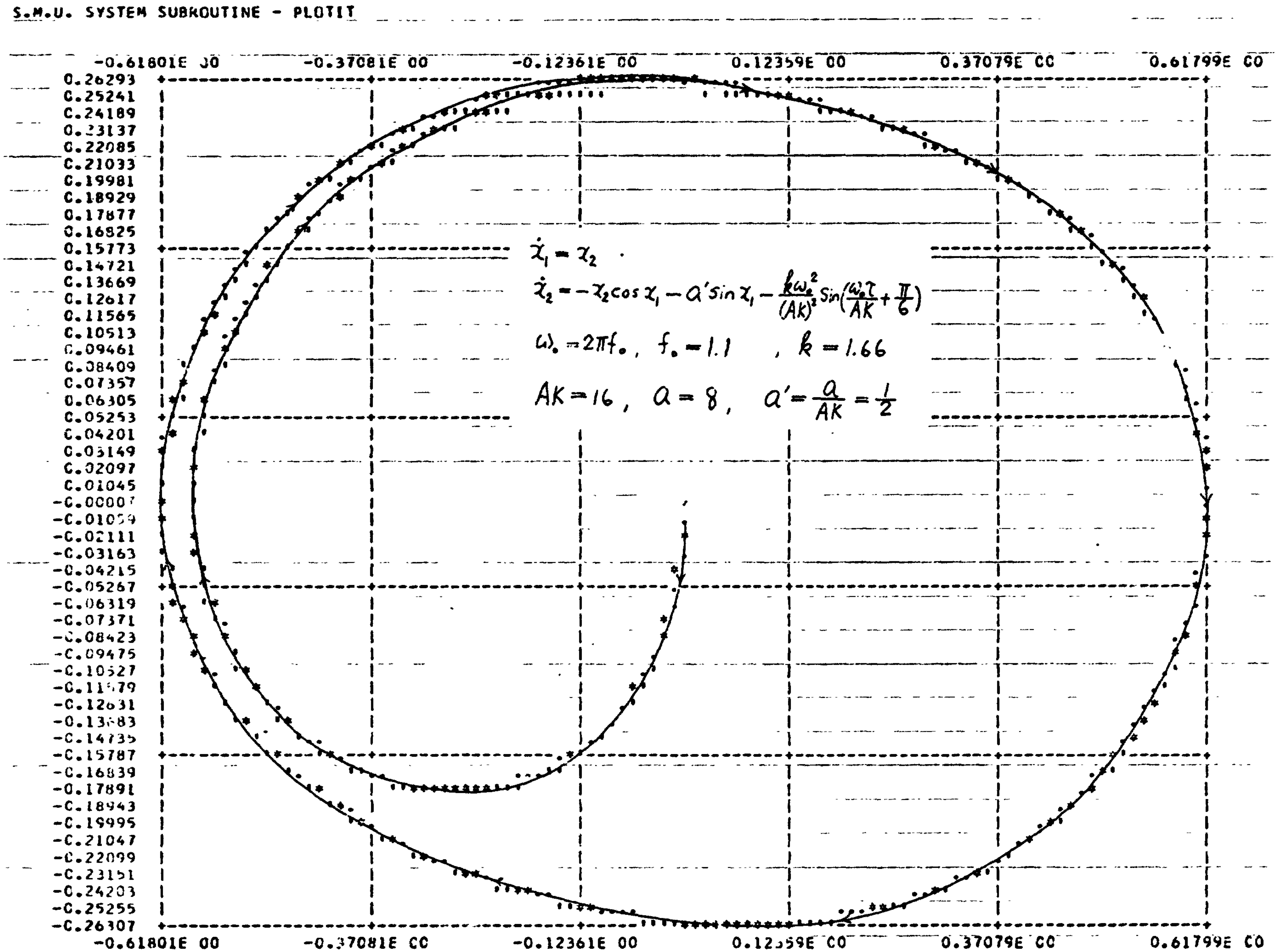
S.M.U. SYSTEM SUBROUTINE - PLOTIT
-0.61801E 00
-0.37081E 00
-0.12361E 00
0.12359E 00
0.37079E 00
0.61799E 00
0.26293
-0.26307
$\dot{x}_1 = x_2$
$\dot{x}_2 = -x_2 \cos x_1 - a' \sin x_1 - \frac{k\omega_0^2}{(AK)^2} \sin\left(\frac{\omega_0 \tau}{AK} + \frac{\pi}{6}\right)$
$\omega_0 = 2\pi f_0$, $f_0 = 1.1$, $k = 1.66$
$AK = 16$, $a = 8$, $a' = \frac{a}{AK} = \frac{1}{2}$

Fig. 2(a)

S.M.U. SYSTEM SUBROUTINE - PLOTIT

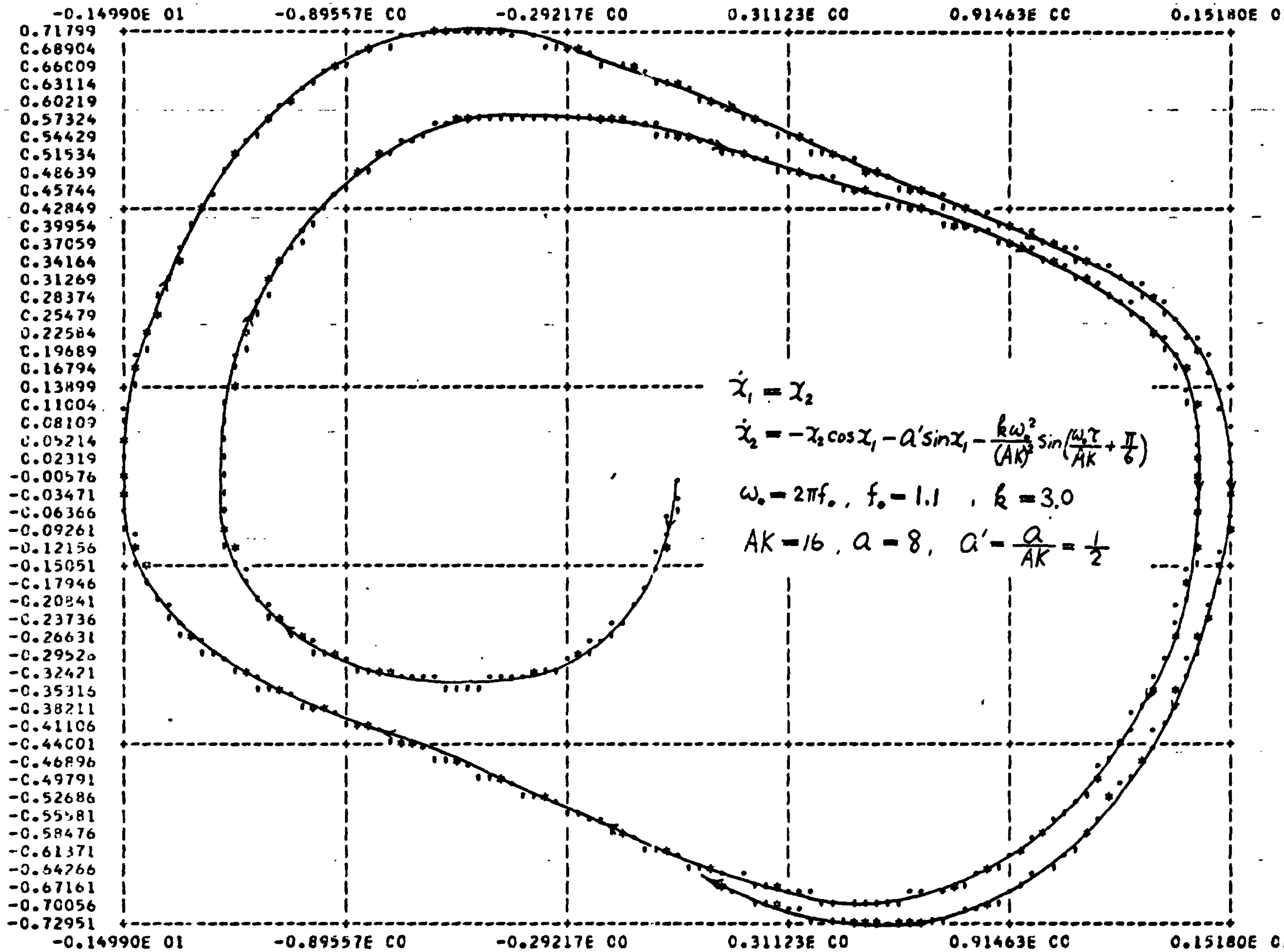

Fig. 2(b)

S.M.U. SYSTEM SUBROUTINE - PLOTIT

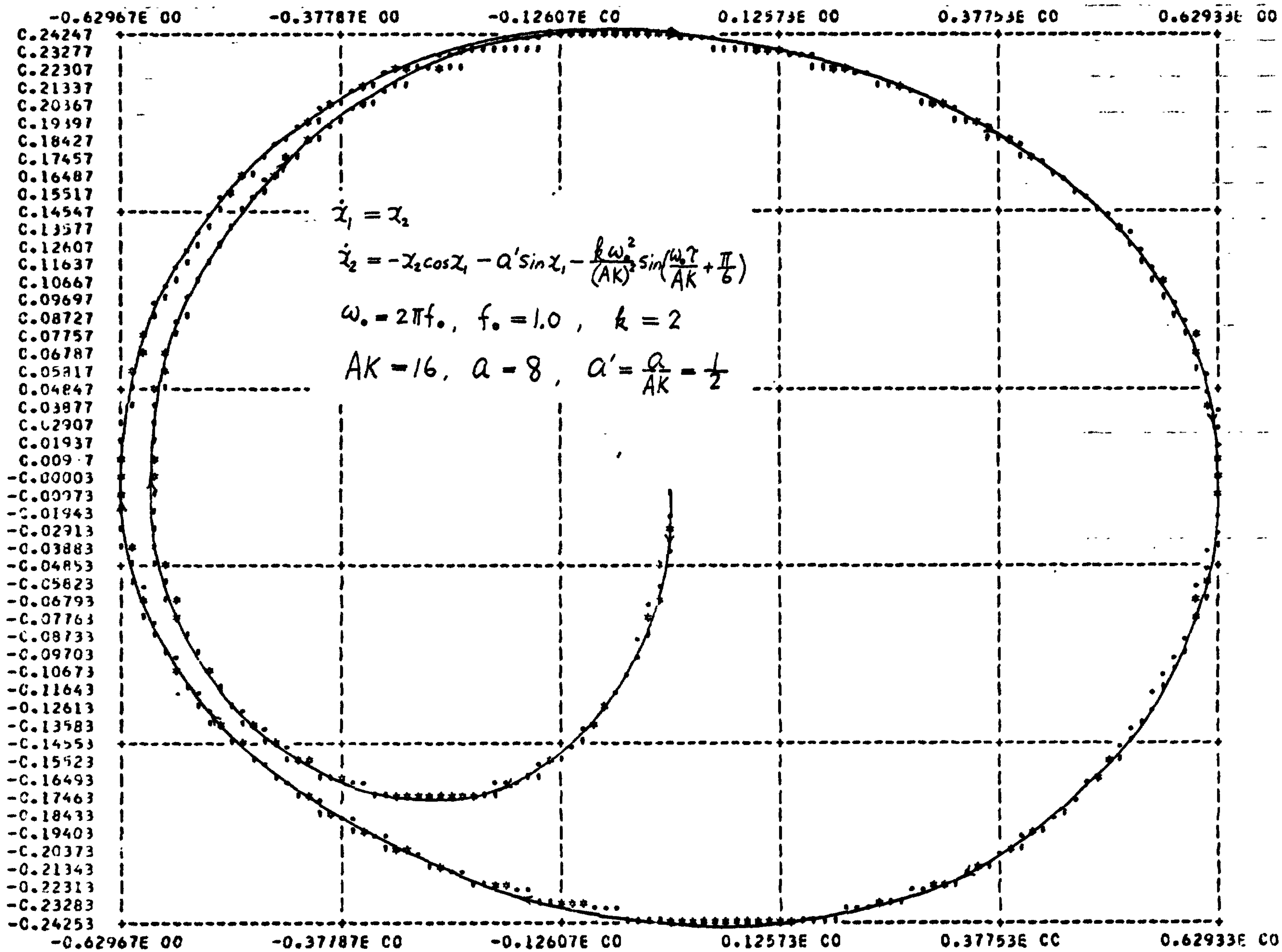

Fig. 3(a)

S.M.U. SYSTEM SUBROUTINE - PLOTIT

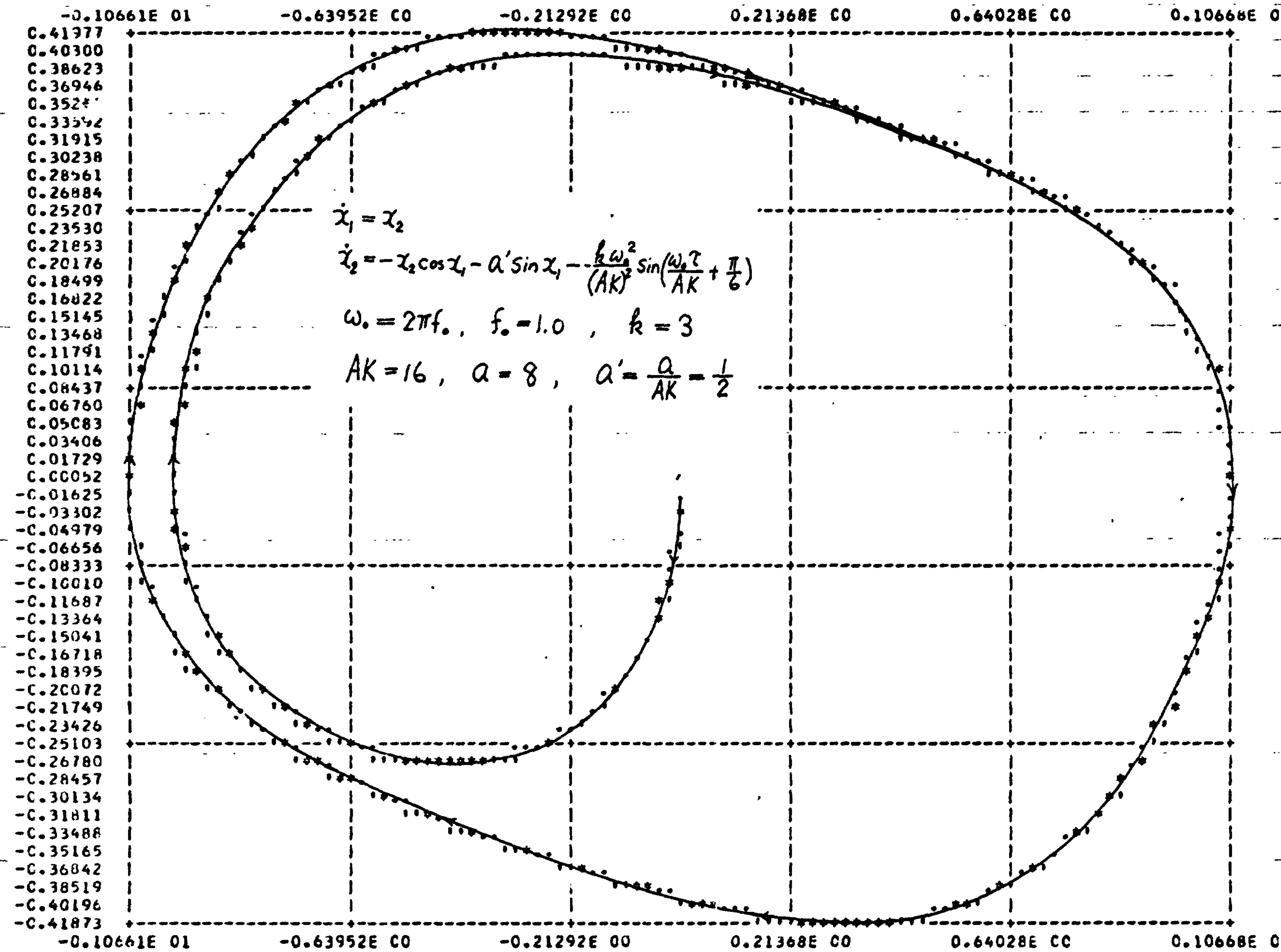

Fig. 3(b)

S.M.U. SYSTEM SUBROUTINE - PLOTIT

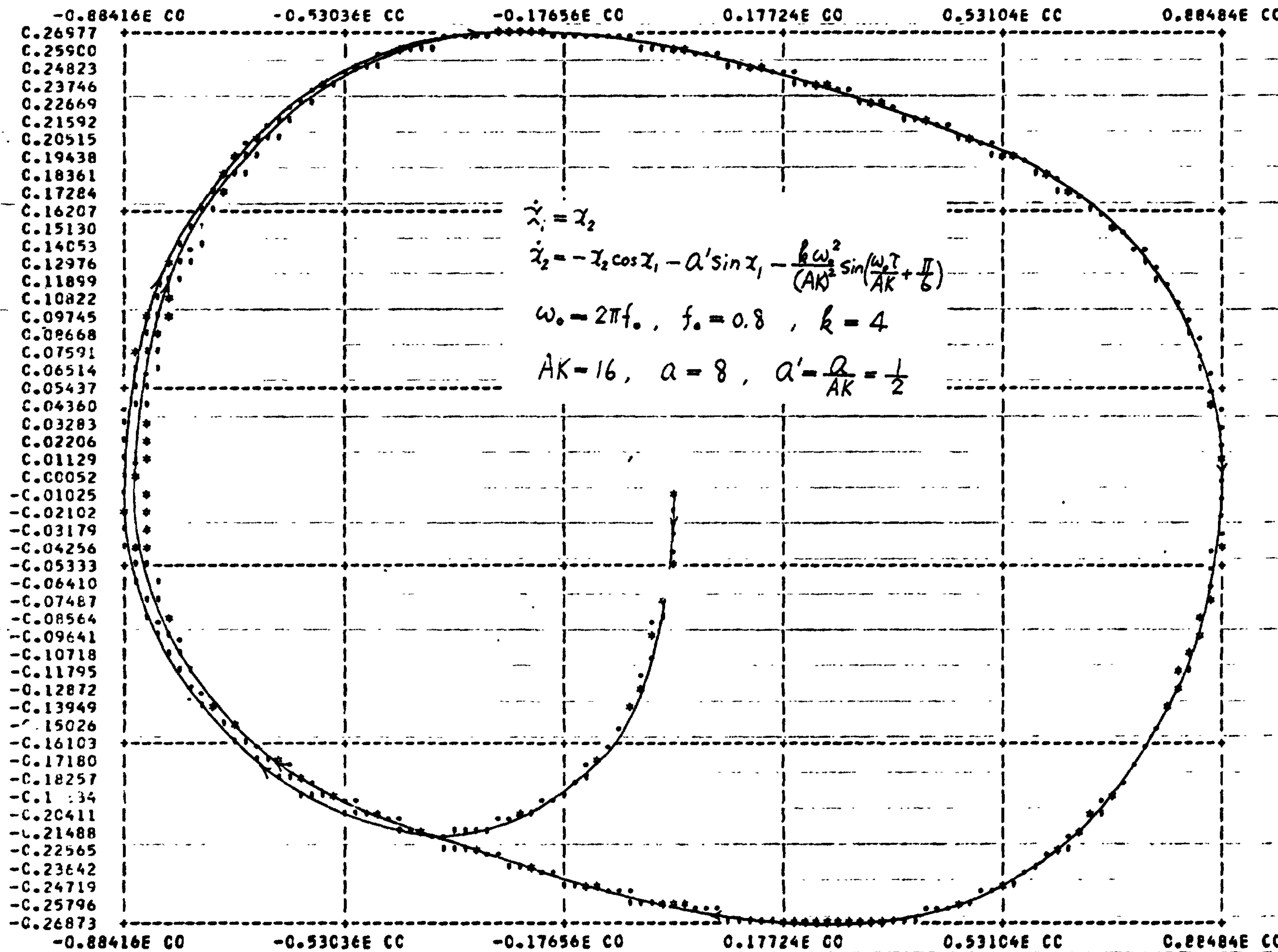

Fig. 4(a)

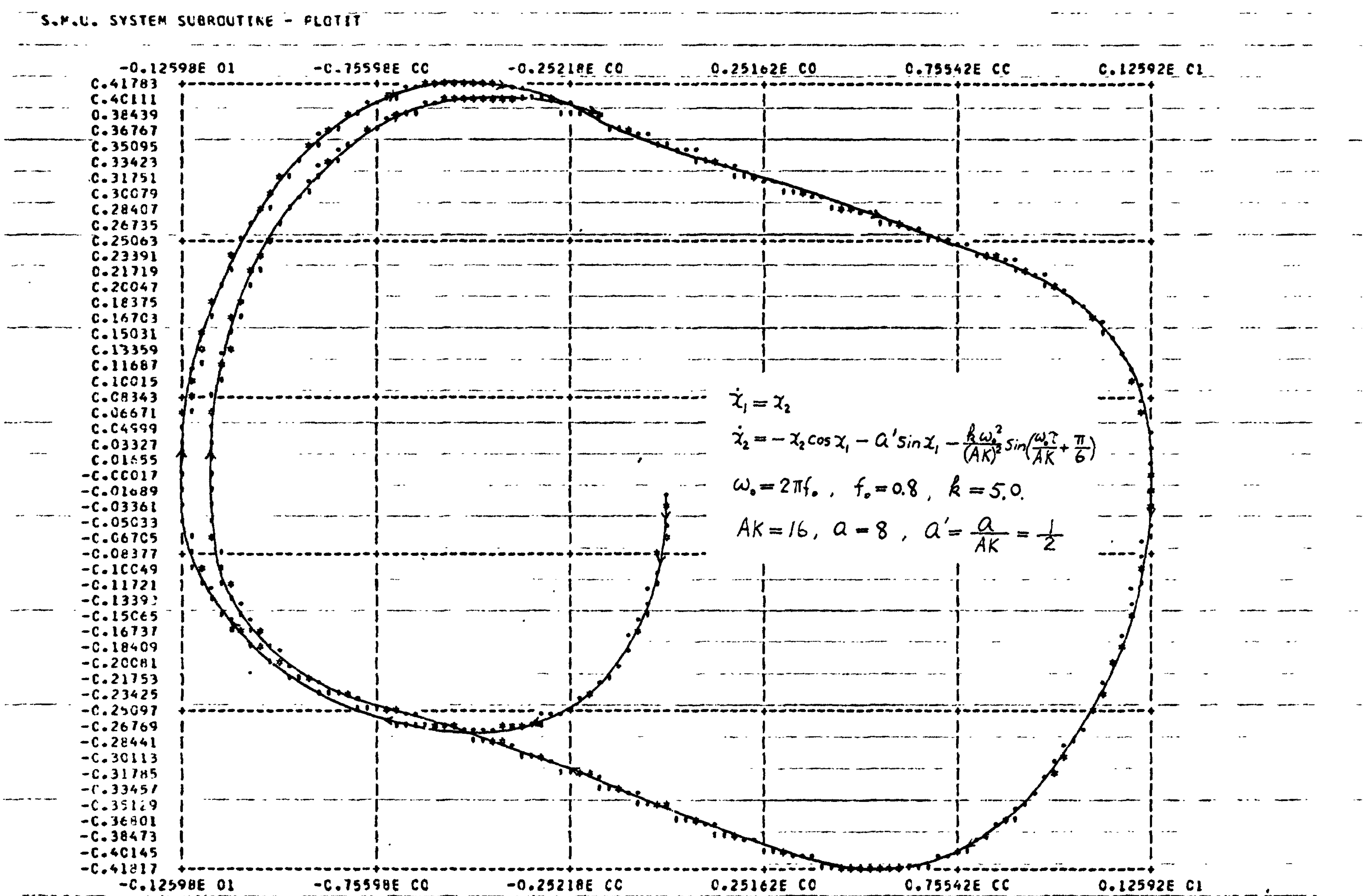
S.M.U. SYSTEM SUBROUTINE - PLOTIT
-0.12598E 01
-0.75598E 00
-0.25218E 00
0.25162E 00
0.75542E 00
0.12592E 01
0.41783
0.40111
0.38439
0.36767
0.35095
0.33423
0.31751
0.30079
0.28407
0.26735
0.25063
0.23391
0.21719
0.20047
0.18375
0.16703
0.15031
0.13359
0.11687
0.10015
0.08343
0.06671
0.04999
0.03327
0.01655
-0.00017
-0.01689
-0.03361
-0.05033
-0.06705
-0.08377
-0.10049
-0.11721
-0.13393
-0.15065
-0.16737
-0.18409
-0.20081
-0.21753
-0.23425
-0.25097
-0.26769
-0.28441
-0.30113
-0.31785
-0.33457
-0.35129
-0.36801
-0.38473
-0.40145
-0.41817
$\dot{x}_1 = x_2$
$\dot{x}_2 = -x_2 \cos x_1 - a' \sin x_1 - \frac{k\omega_0^2}{(AK)^2} \sin\left(\frac{\omega_0 \tau}{AK} + \frac{\pi}{6}\right)$
$\omega_0 = 2\pi f_0$, $f_0 = 0.8$, $k = 5.0$
$AK = 16$, $a = 8$, $a' = \frac{a}{AK} = \frac{1}{2}$

Fig. 4 (b)

S.M.U. SYSTEM SUBROUTINE - PLOTIT

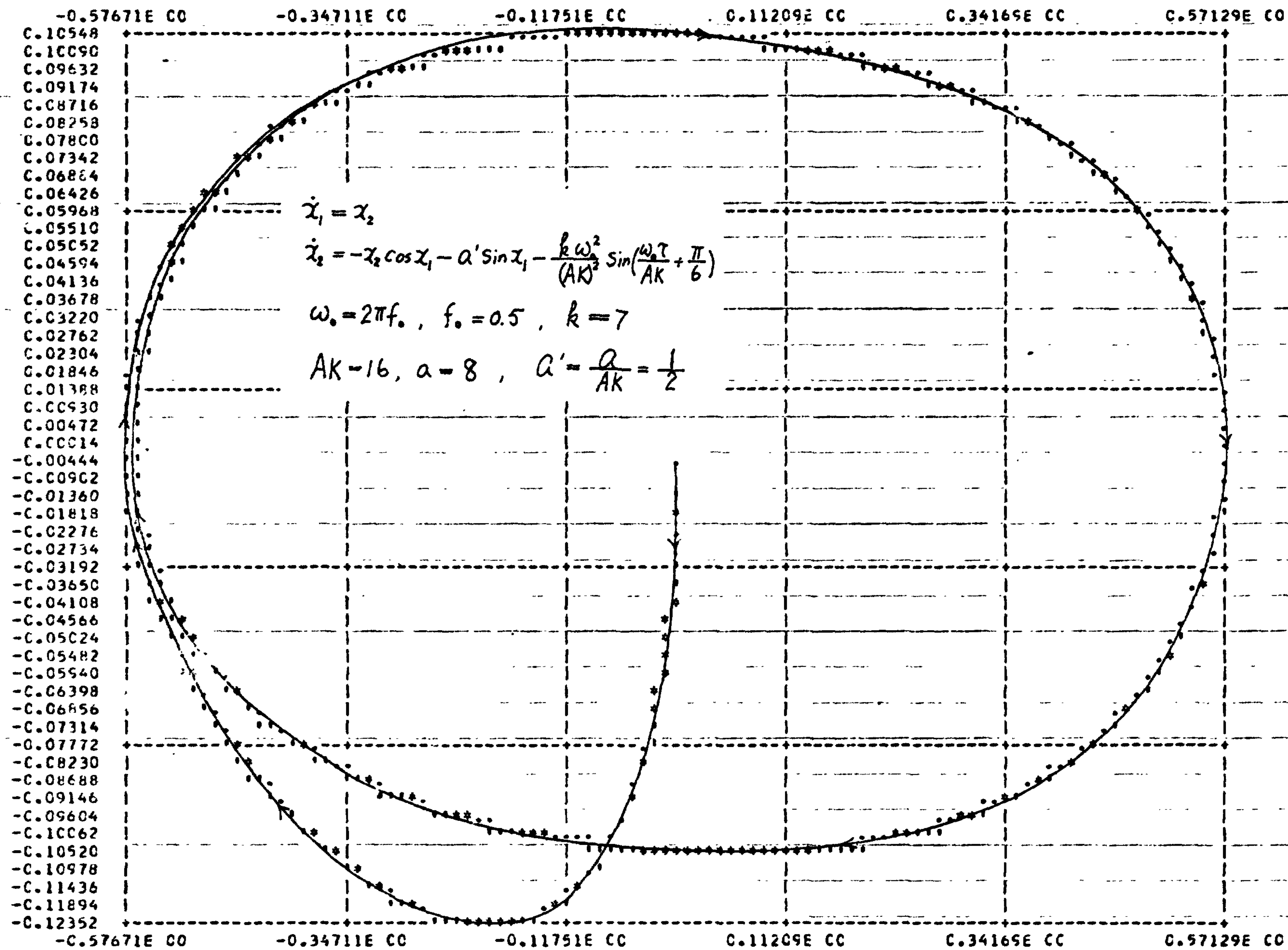

Fig. 5(a)

S.M.U. SYSTEM SUBROUTINE - PLOTIT

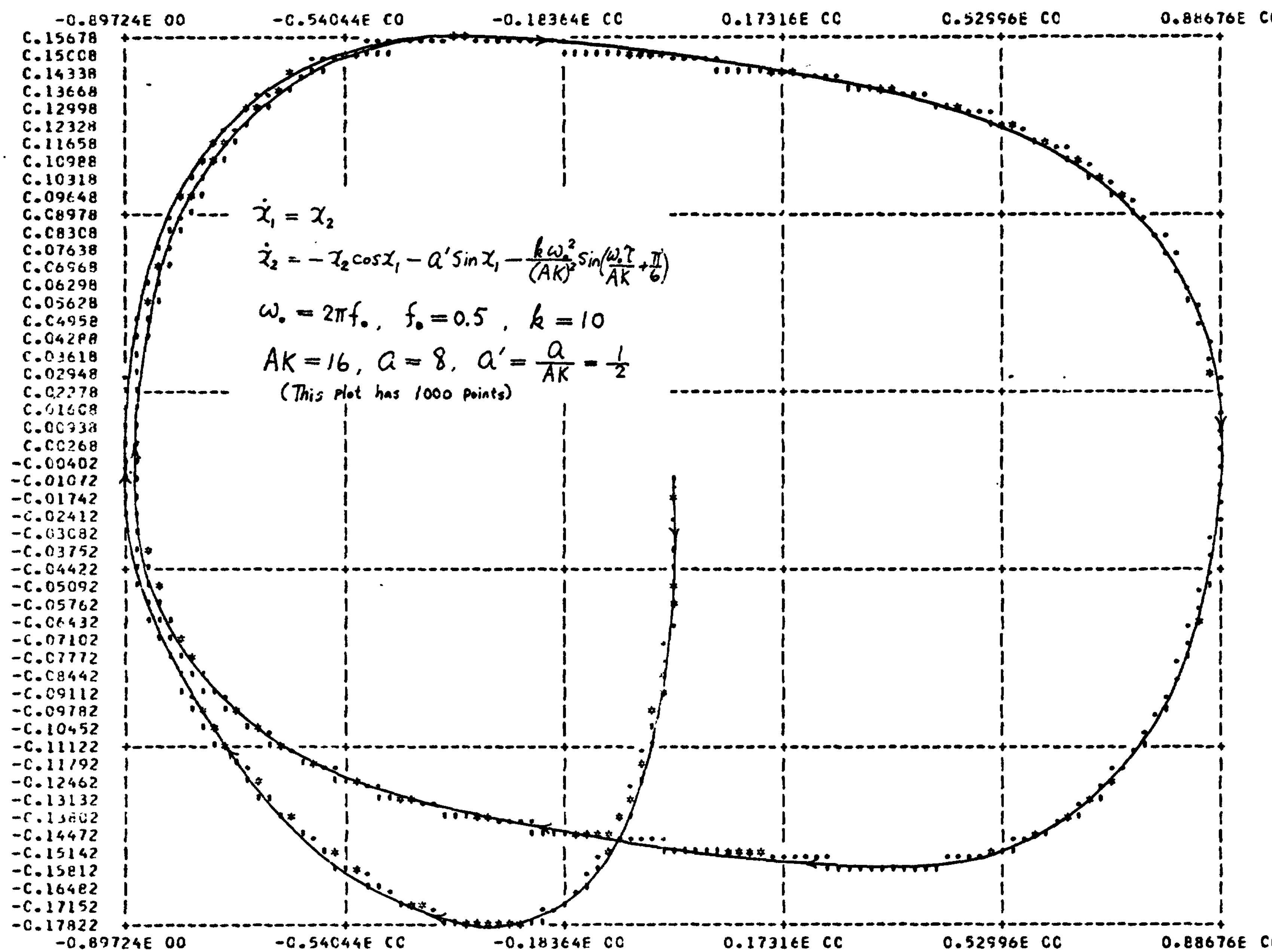

Fig. 5 (b)

S.M.U. SYSTEM SUBROUTINE - PLOTIT

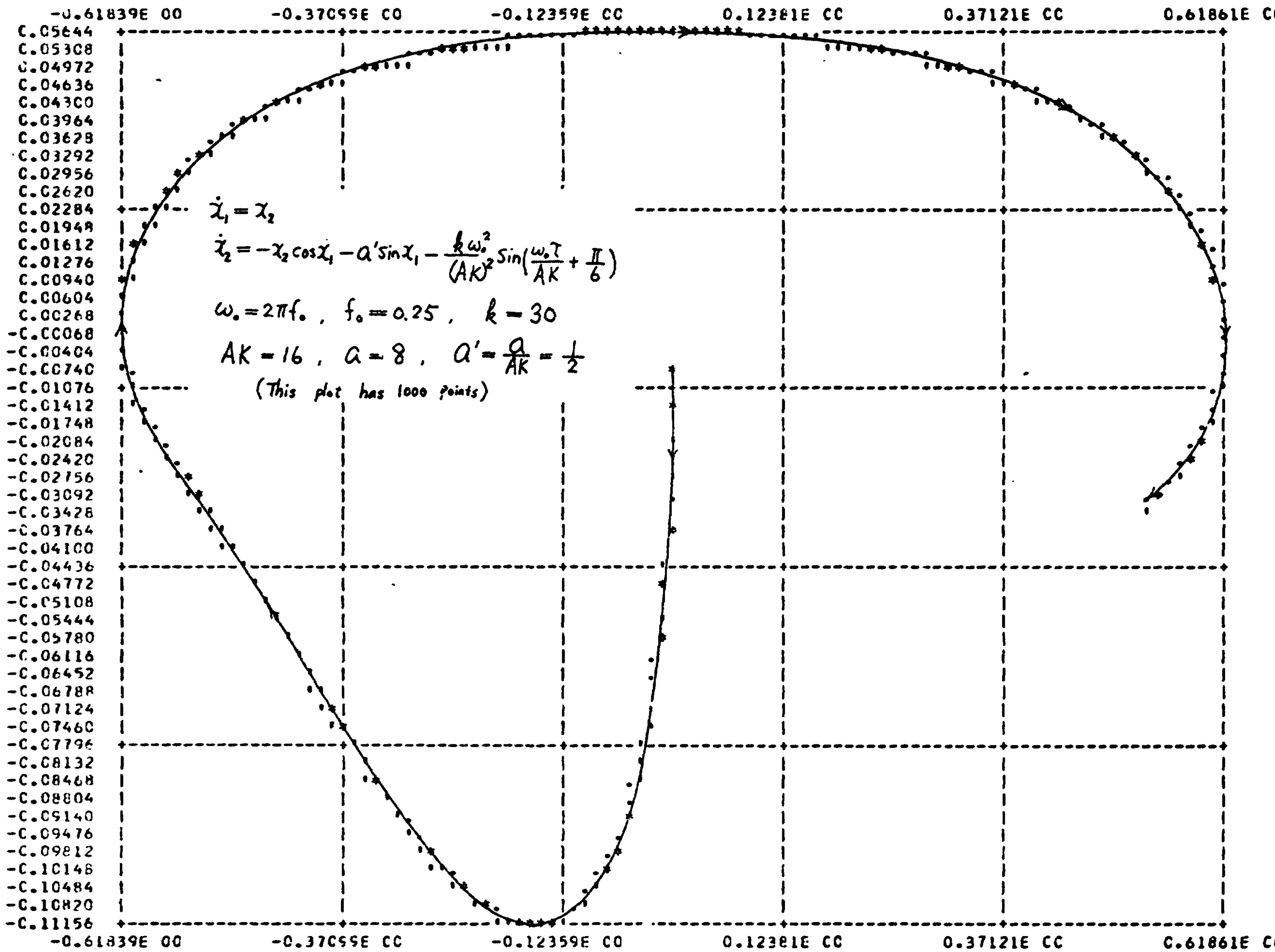

Fig. 6(a)

S.M.U. SYSTEM SUBROUTINE - PLOTIT

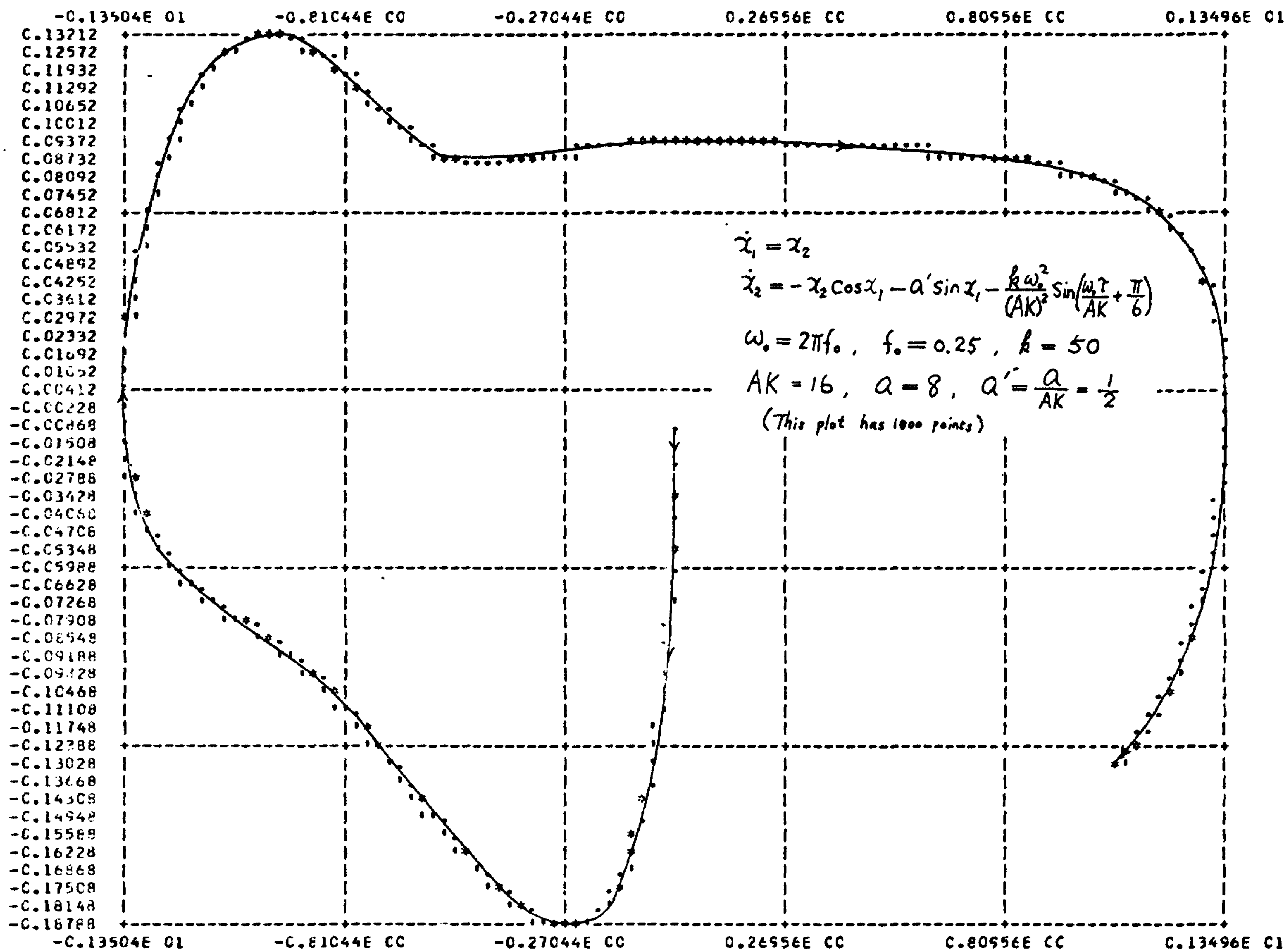

Fig. 6(b)

S.M.U. SYSTEM SUBROUTINE - PLOTIT

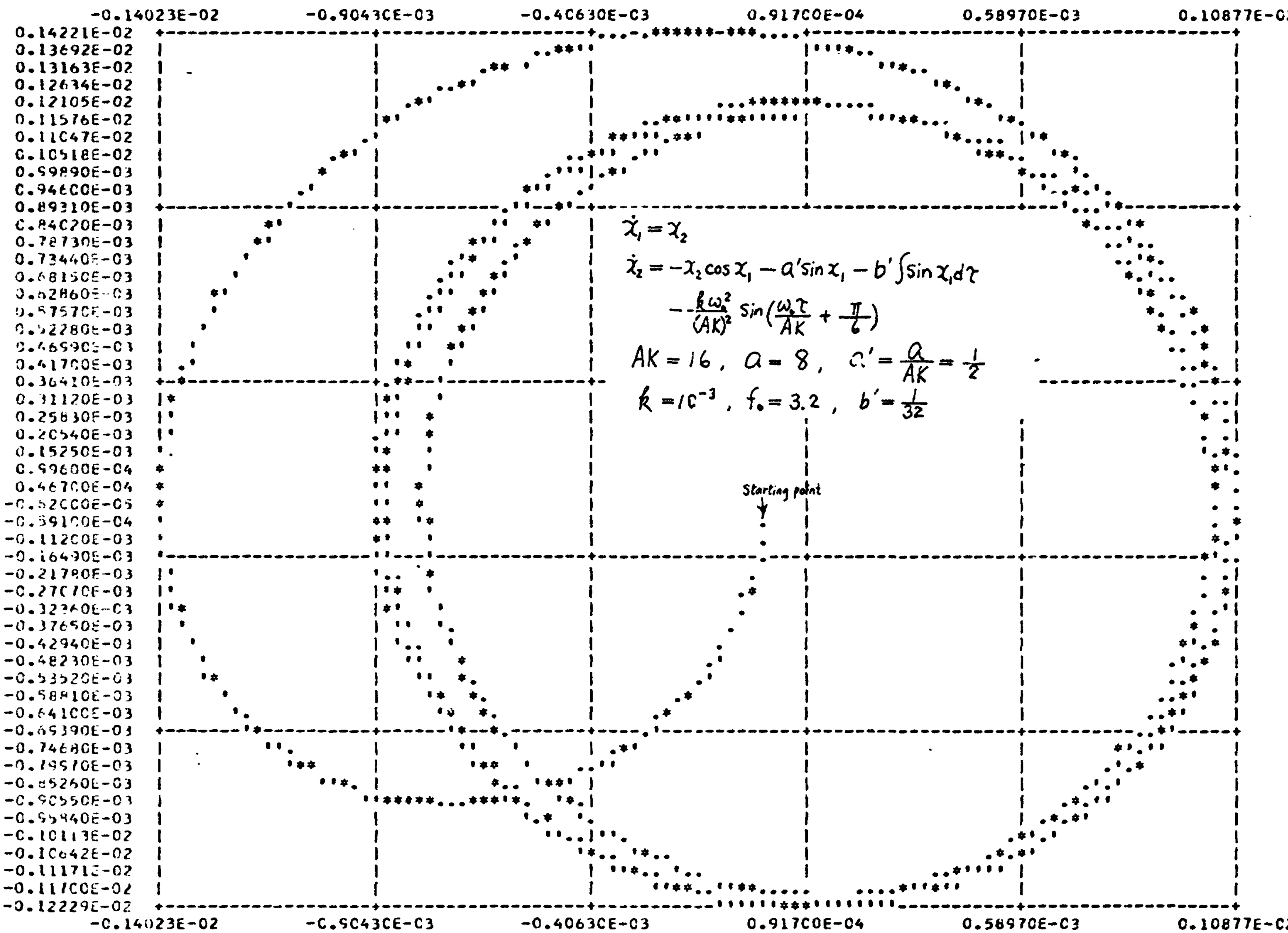

Fig. 7(a)

S.M.U. SYSTEM SUBROUTINE - PLOTIT

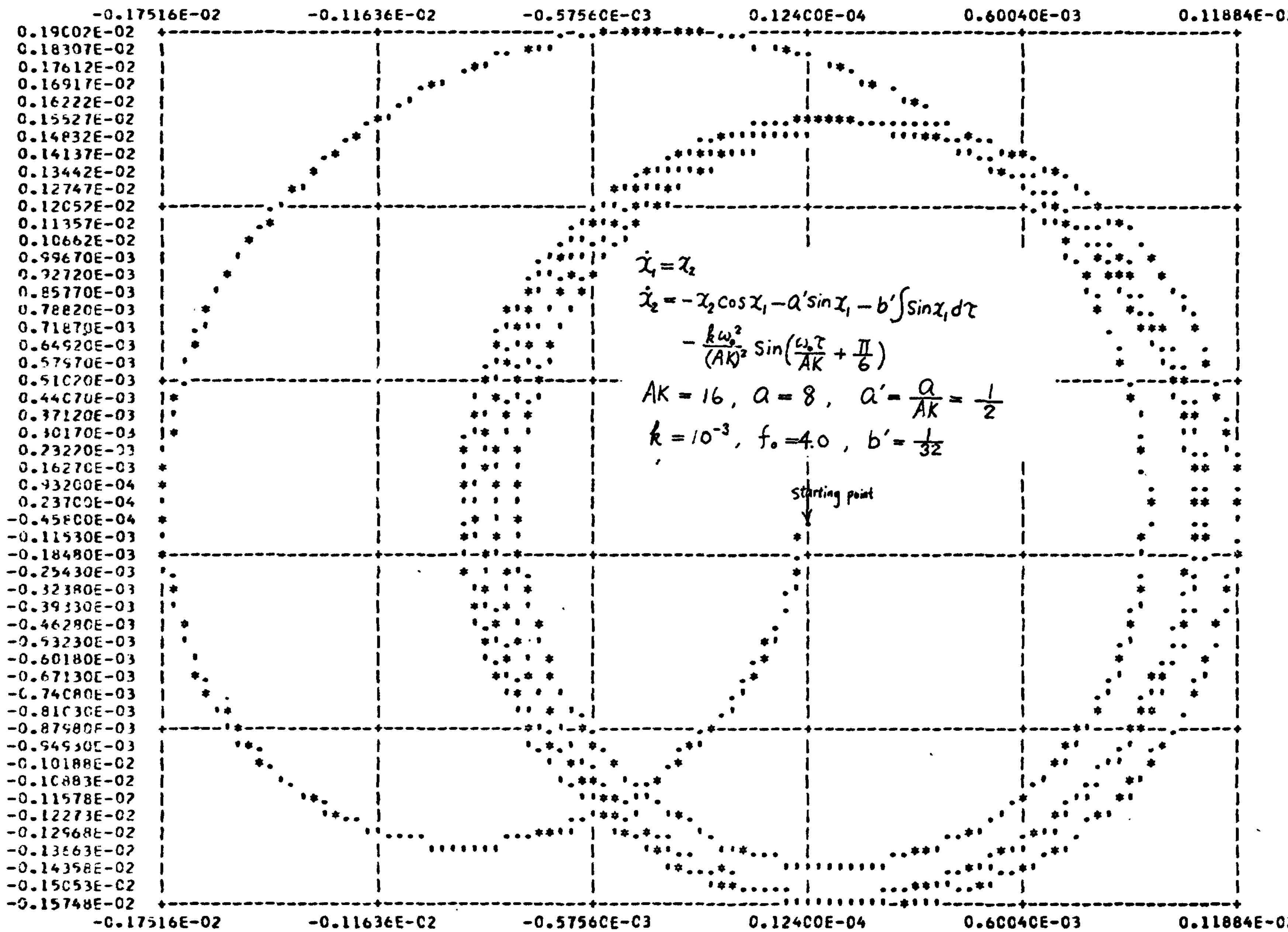

Fig. 7(b)

S.M.U. SYSTEM SUBROUTINE - PLOTIT

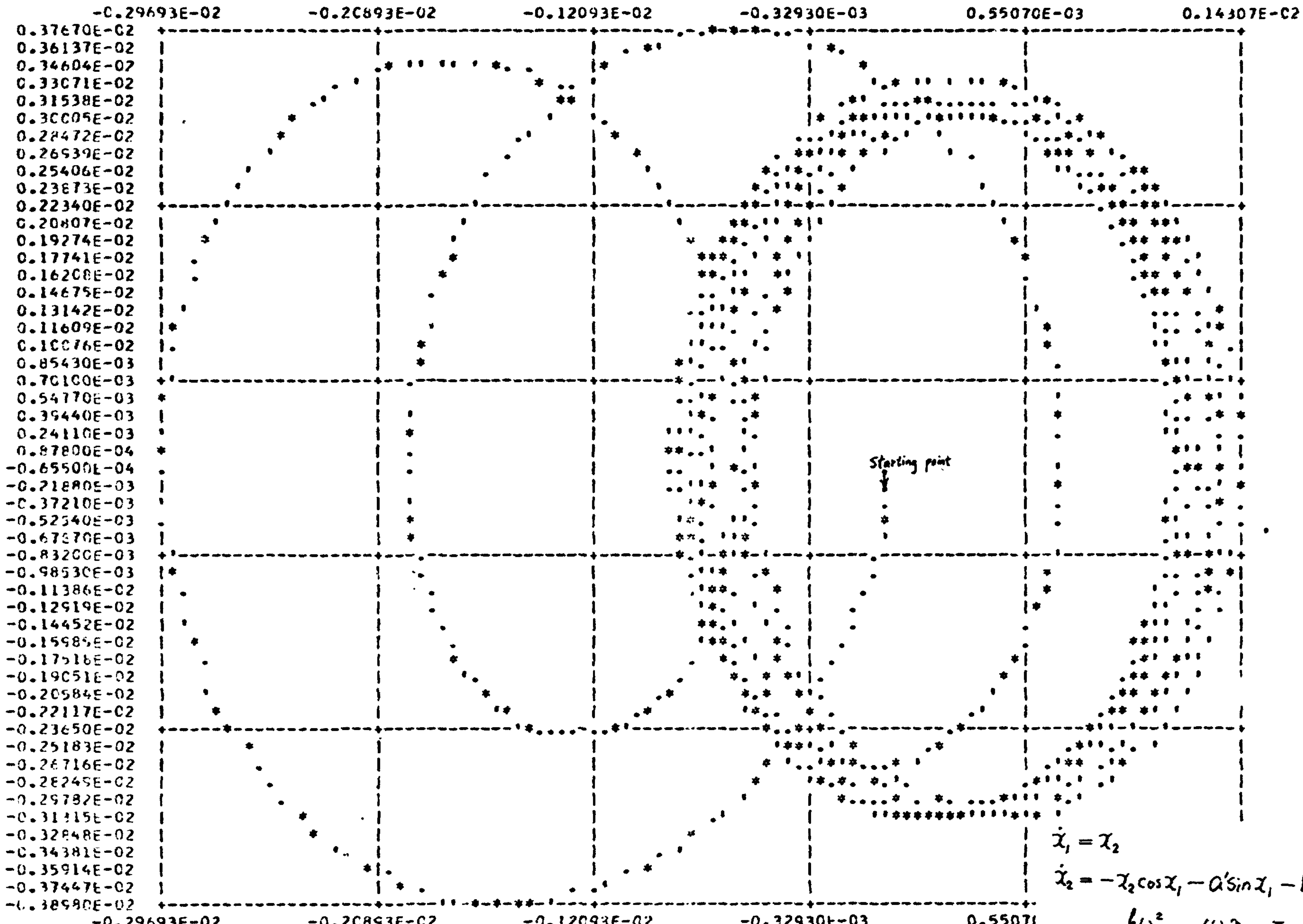

$$\dot{x}_1 = x_2$$

$$\dot{x}_2 = -x_2 \cos x_1 - a' \sin x_1 - b' \int \sin x_1 d\tau - \frac{k\omega_0^2}{(AK)^2} \sin\left(\frac{\omega_0 \tau}{AK} + \frac{\pi}{6}\right)$$

$AK = 16$, $a = 8$, $a' = \frac{a}{AK} = \frac{1}{2}$

$k = 10^{-3}$, $f_0 = 8$, $b' = \frac{1}{32}$

Fig. 7(c)

S.P.U. SYSTEM SUBROUTINE - PLOTIT

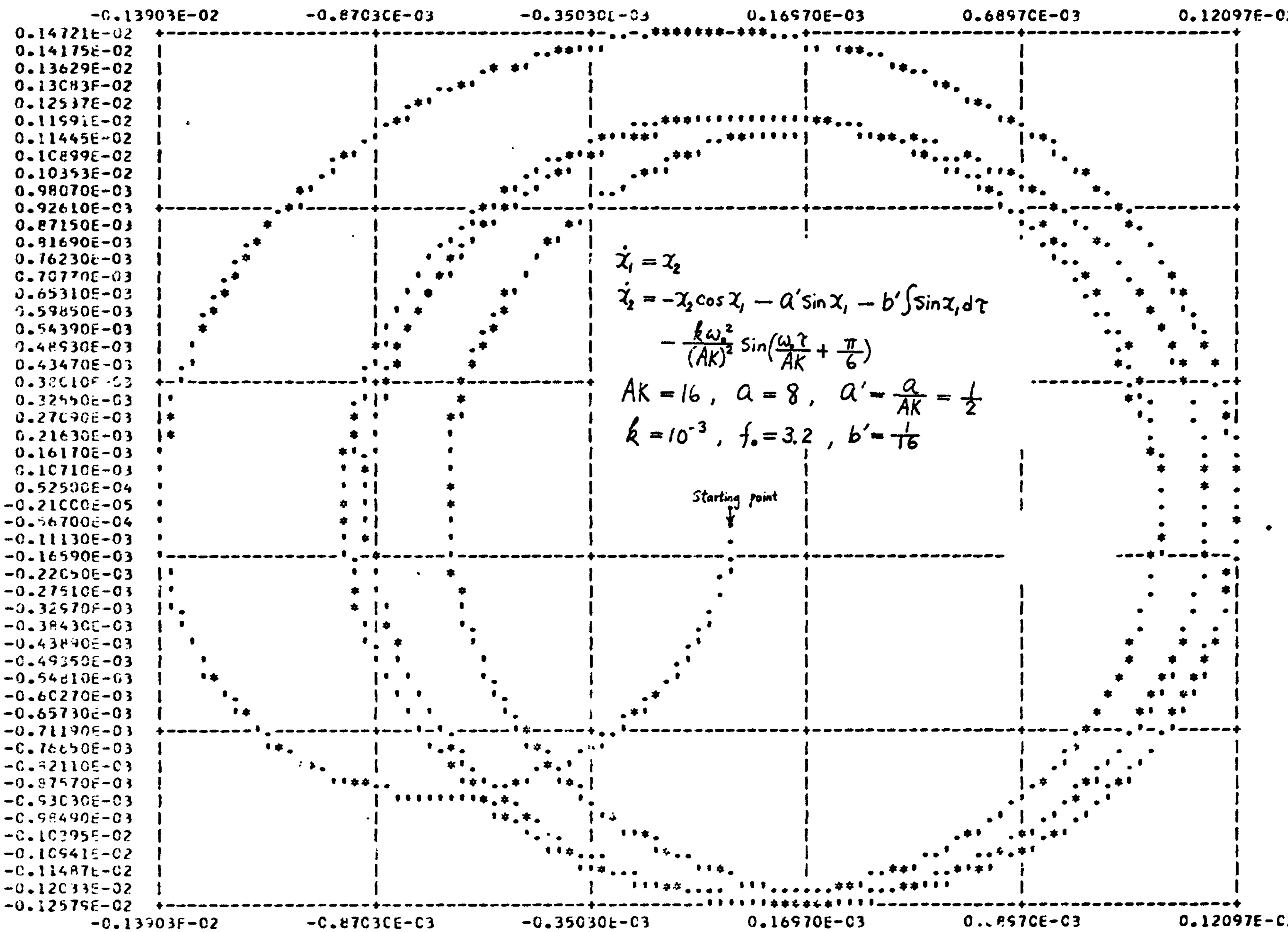

Fig. 8(a)

S.M.U. SYSTEM SUBROUTINE - PLOTIT

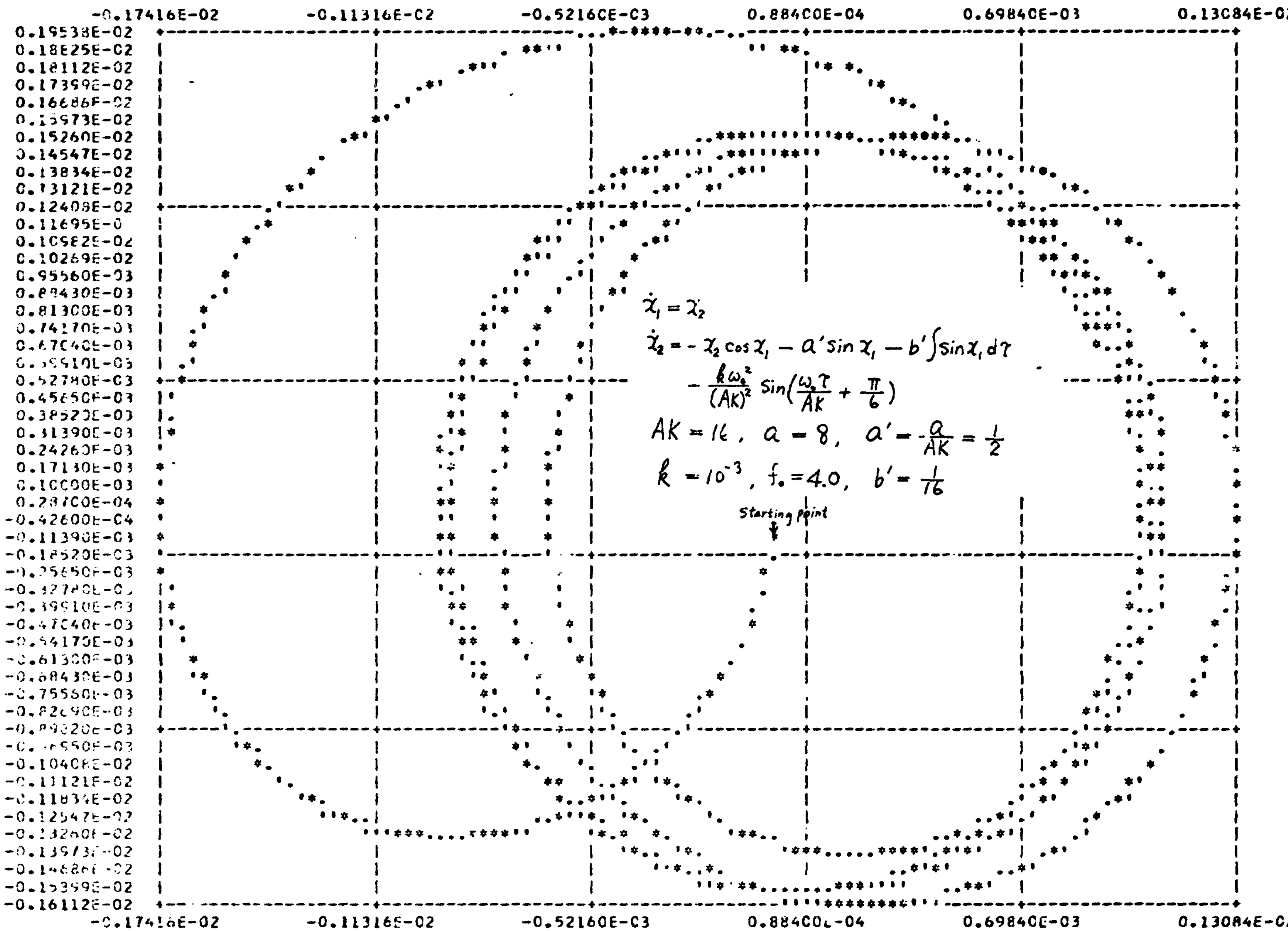

Fig. 8(b)

S.P.U. SYSTEM SUBROUTINE - PLOTIT

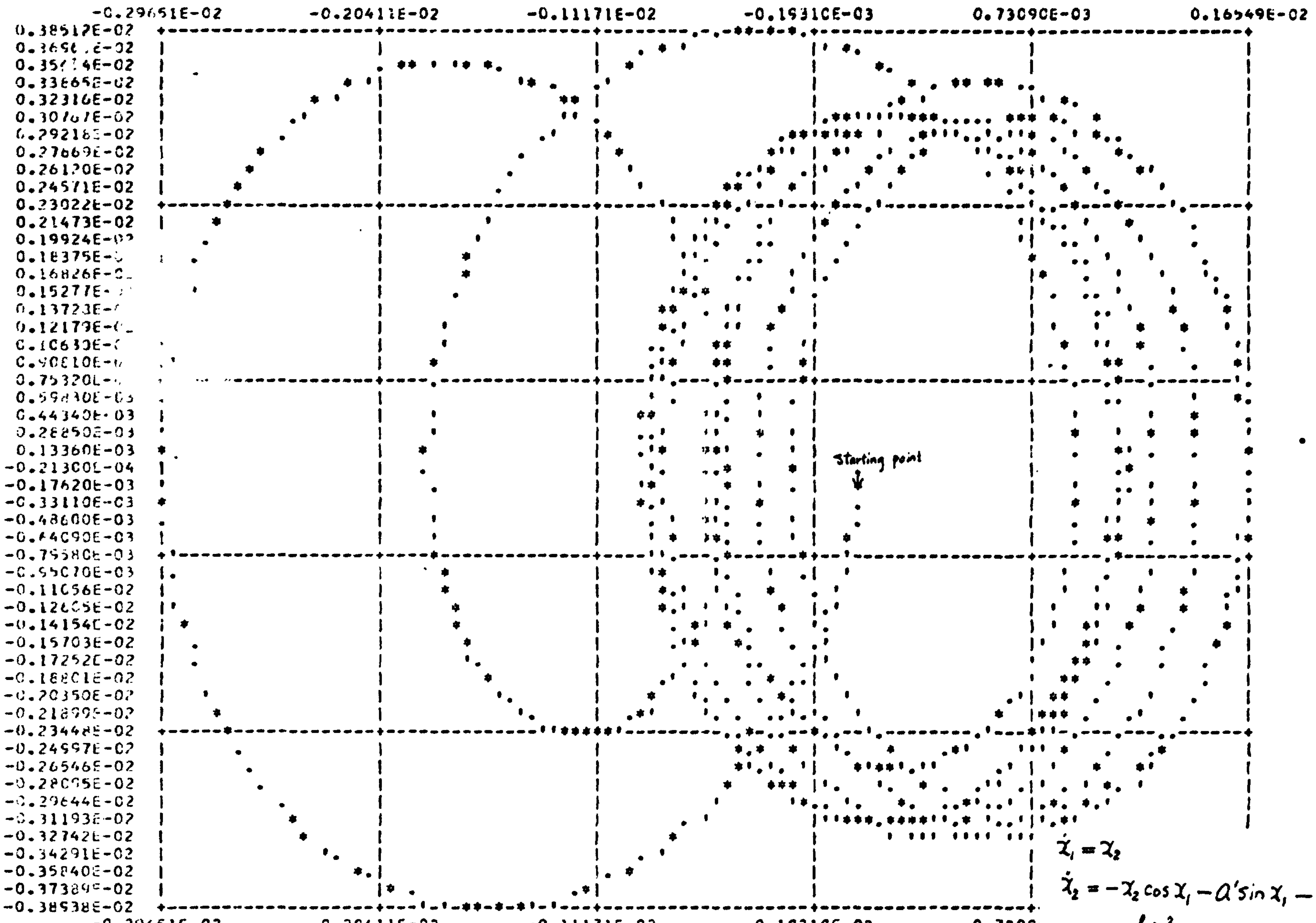

Fig. 8(c)

$\dot{x}_1 = x_2$

$$\dot{x}_2 = -x_2\cos x_1 - a'\sin x_1 - b'\int \sin x_1\,d\tau - \frac{k\omega_0^2}{(AK)^2}\sin\left(\frac{\omega_0\tau}{AK}+\frac{\pi}{6}\right)$$

$AK = 16,\ a = 8,\ a' = \frac{a}{AK} = \frac{1}{2}$

$k = 10^{-3},\ f_0 = 8,\ b' = \frac{1}{16}$

S.P.U. SYSTEM SUBROUTINE - PLOTIT

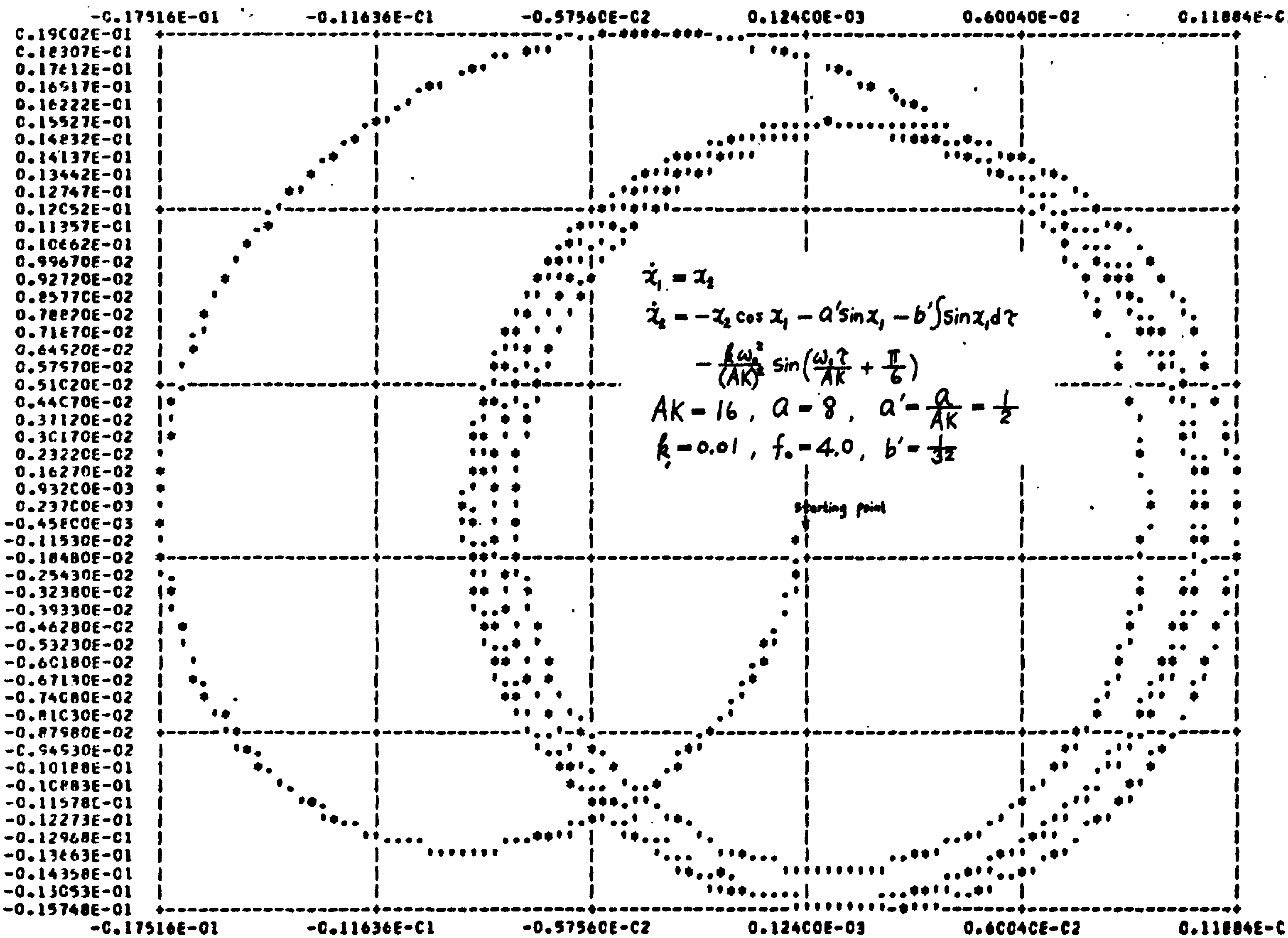

Fig. 9(a)

S.P.U.. SYSTEM SUBROUTINE - PLOTIT

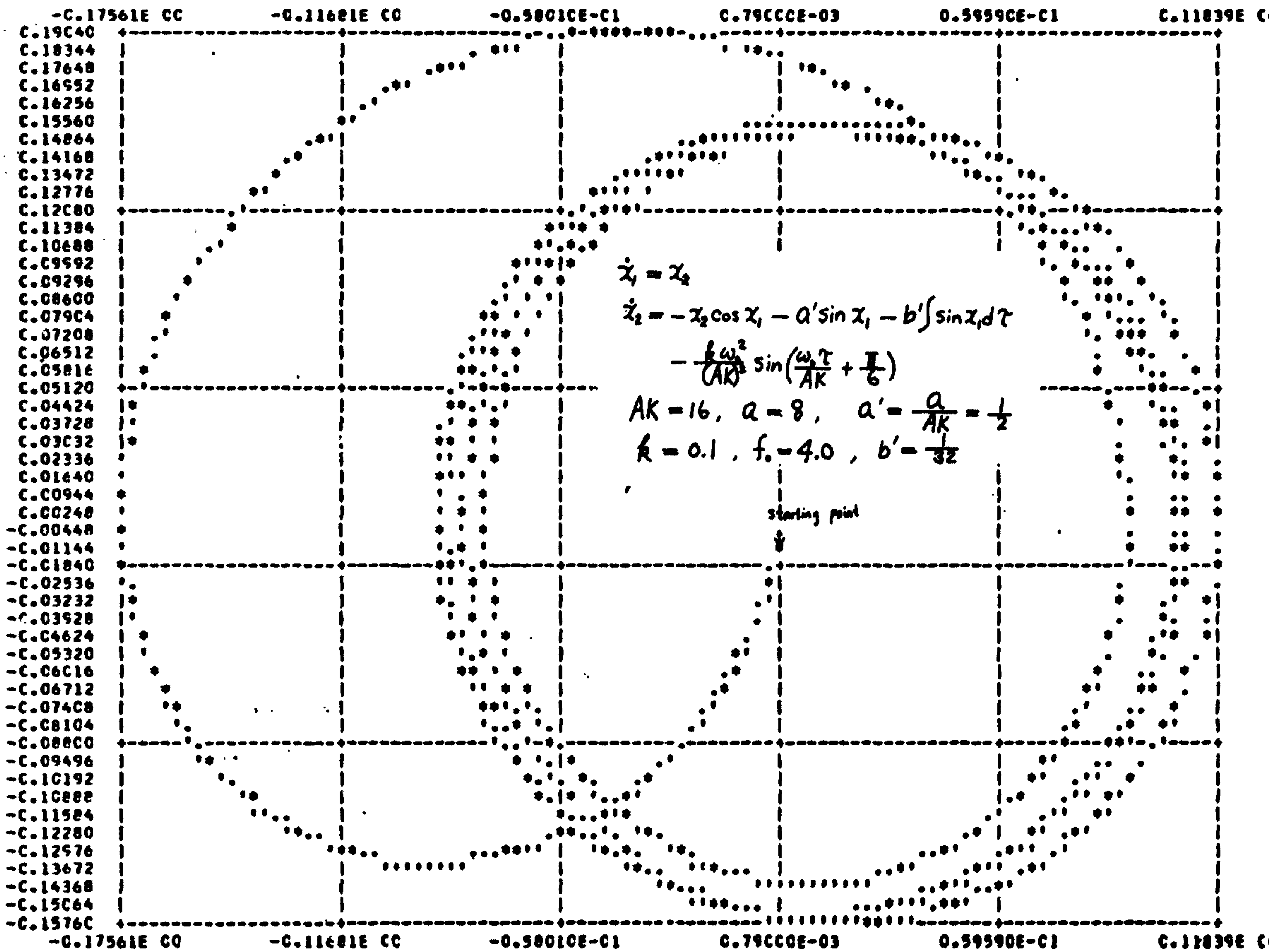

Fig. 9(b)

S.P.U. SUSTEM SUBROUTINE - PLCTIT

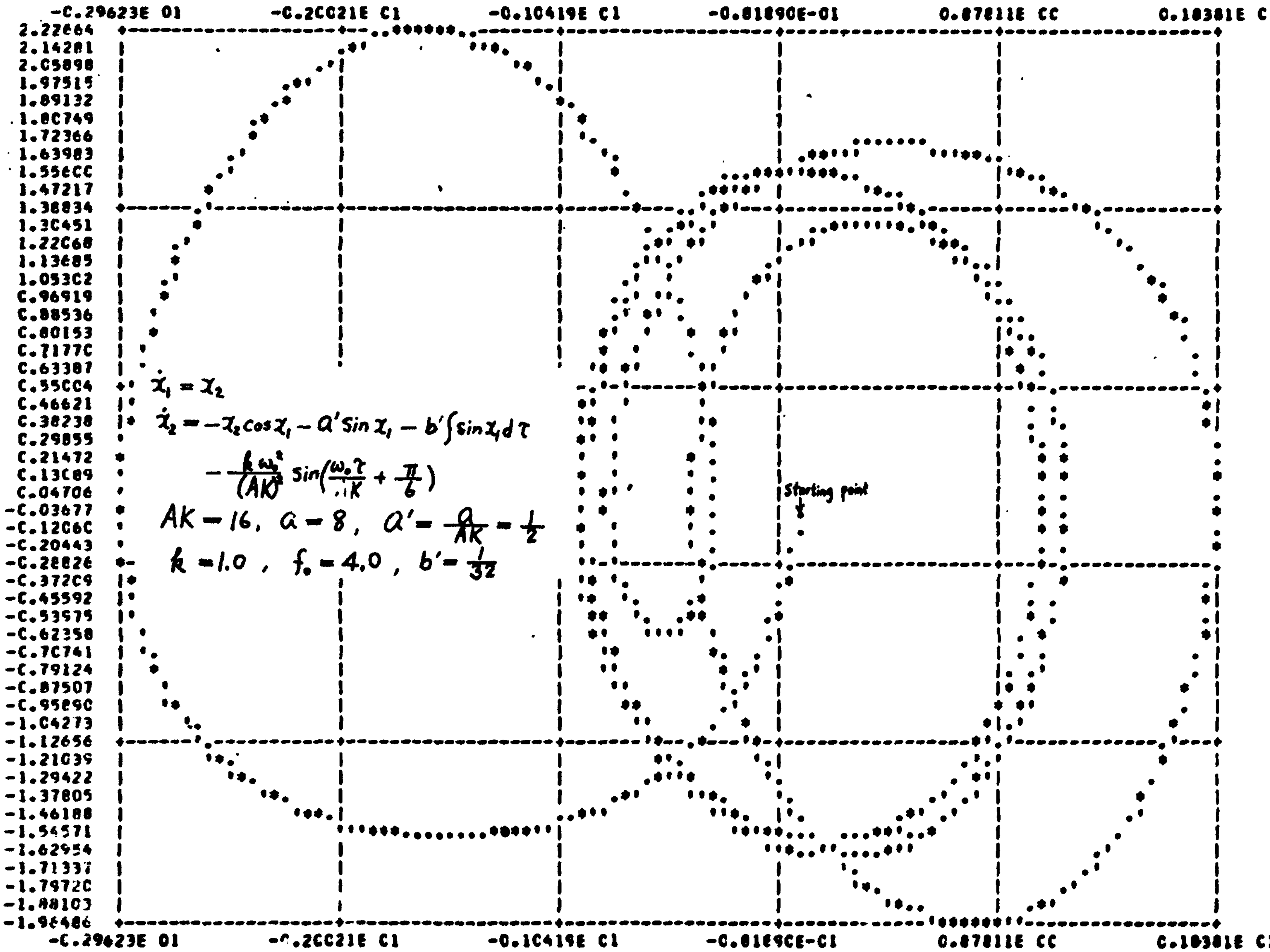

Fig. 9(c)

S.P.L. SYSTEM SUBROUTINE - PLOTIT

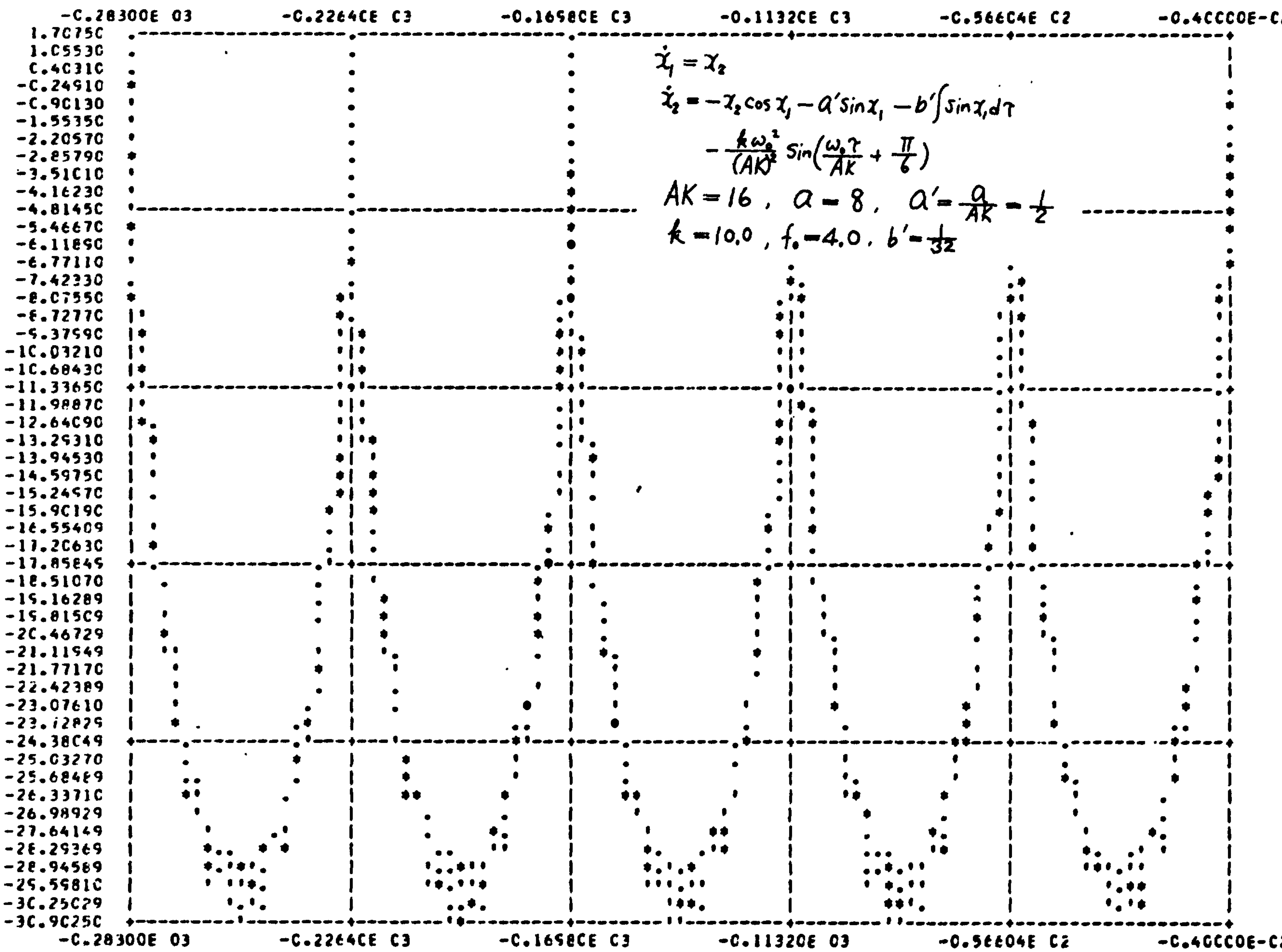

Fig. 9(d)

S.M.U. SYSTEM SUBROUTINE - PLOTIT

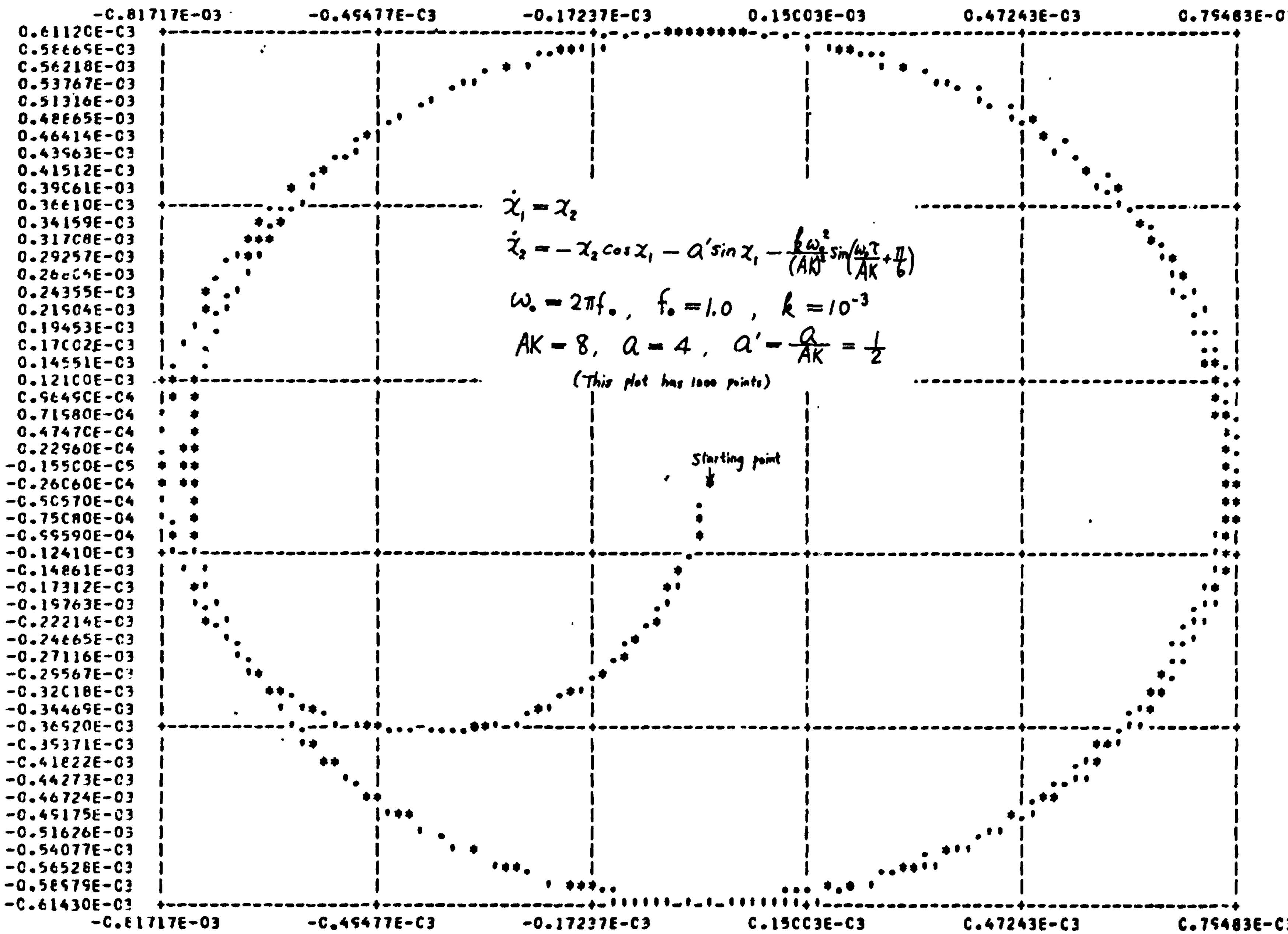

Fig. 10 (a)

S.M.L. SYSTEM SUBROUTINE - PLOTIT

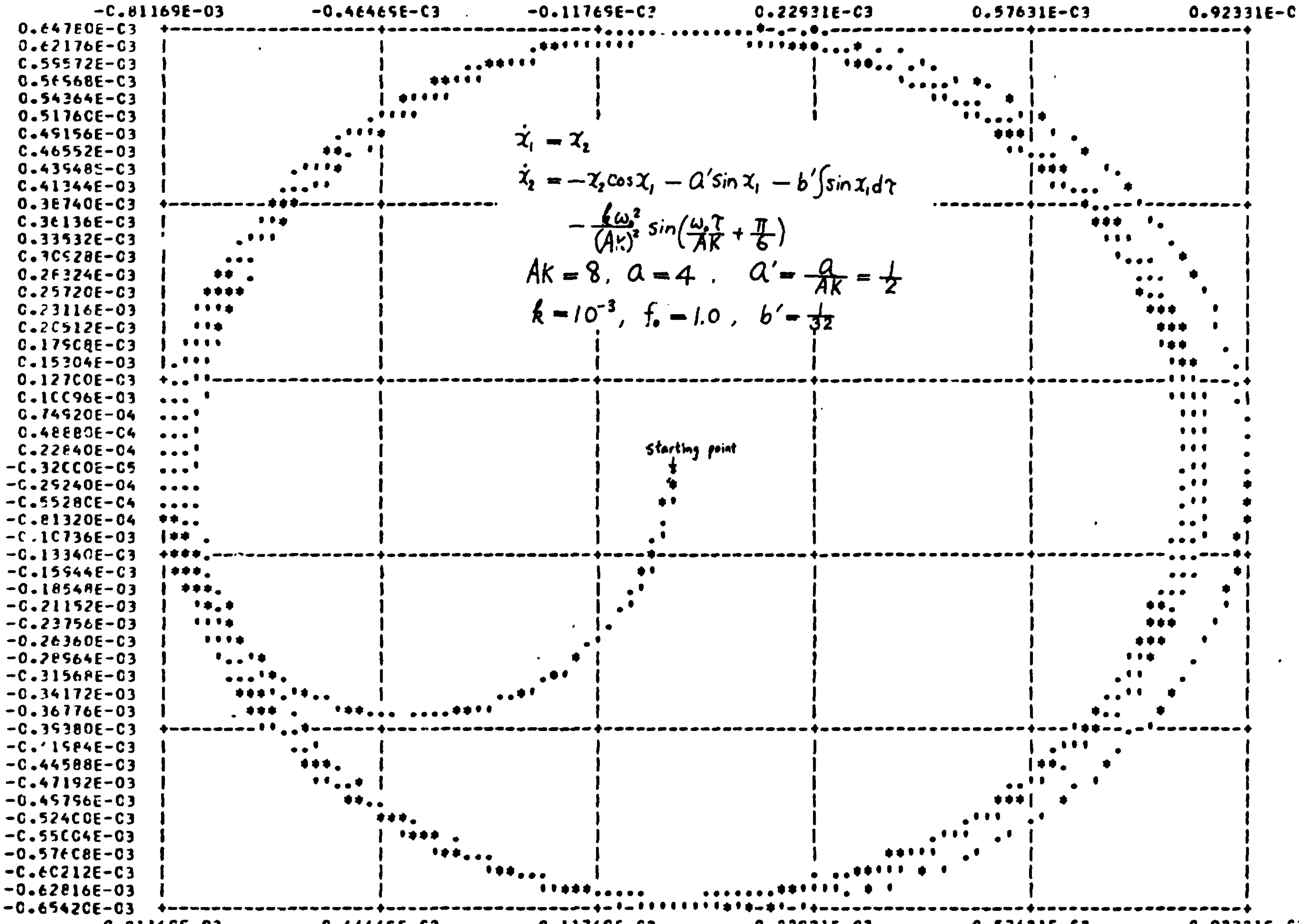

Fig. 10(b)

S.M.U. SYSTEM SUBROUTINE - PLOTIT

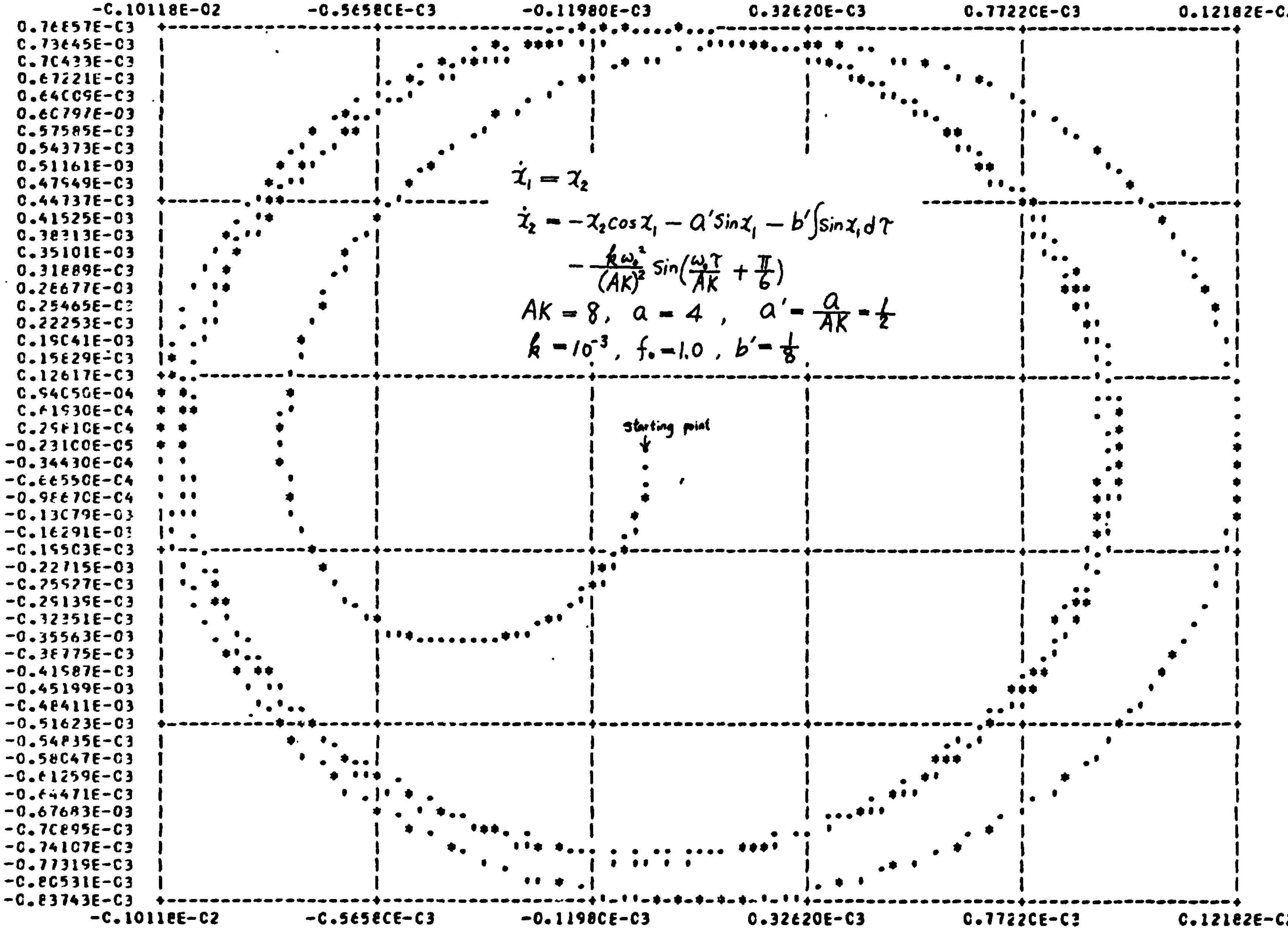

Fig. 10 (c)

S.P.U. SYSTEM SUBROUTINE - PLOTIT

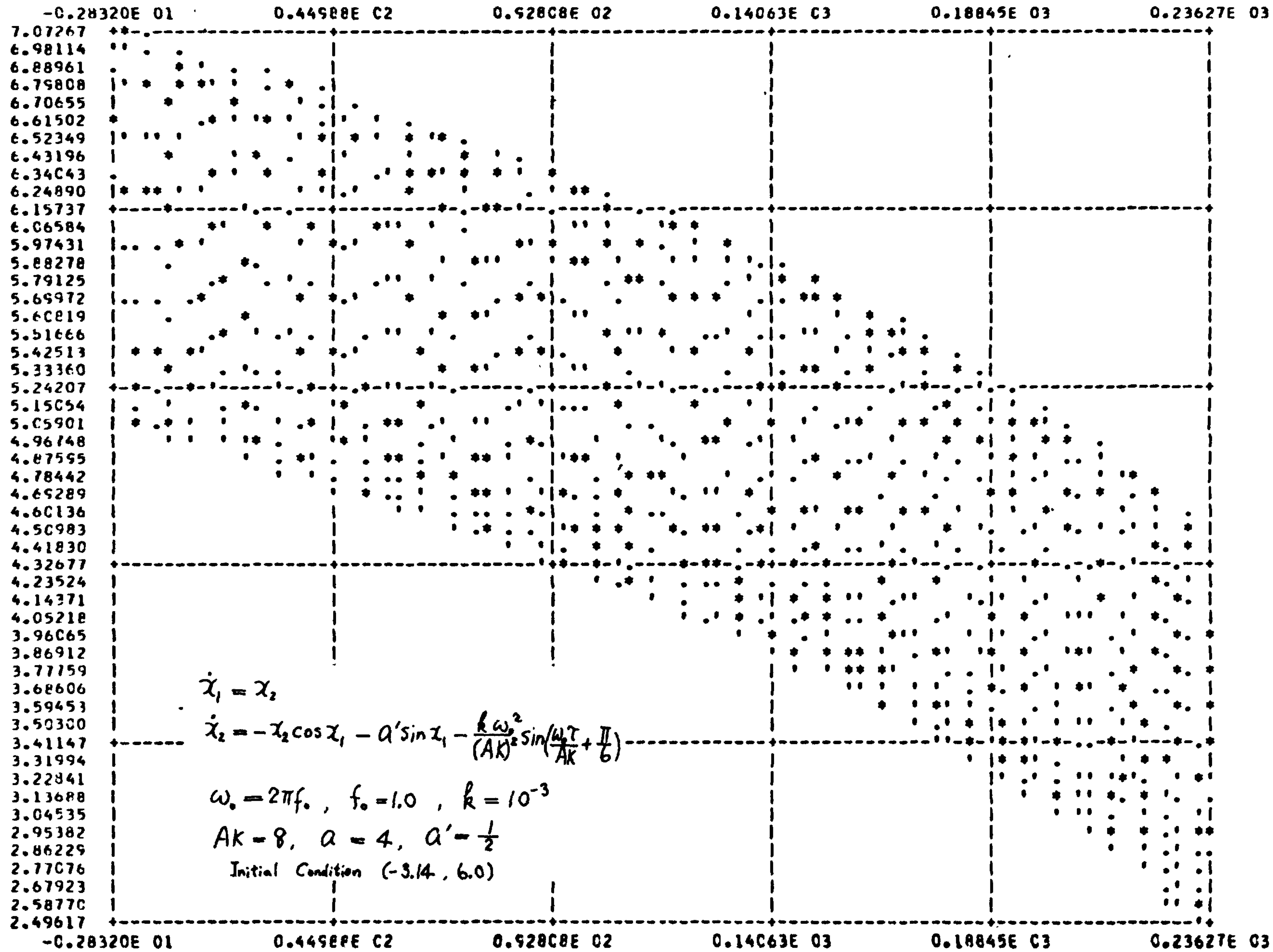

Fig. 11(a)

S.M.U. SYSTEM SUBRCUTINE - PLOTIT

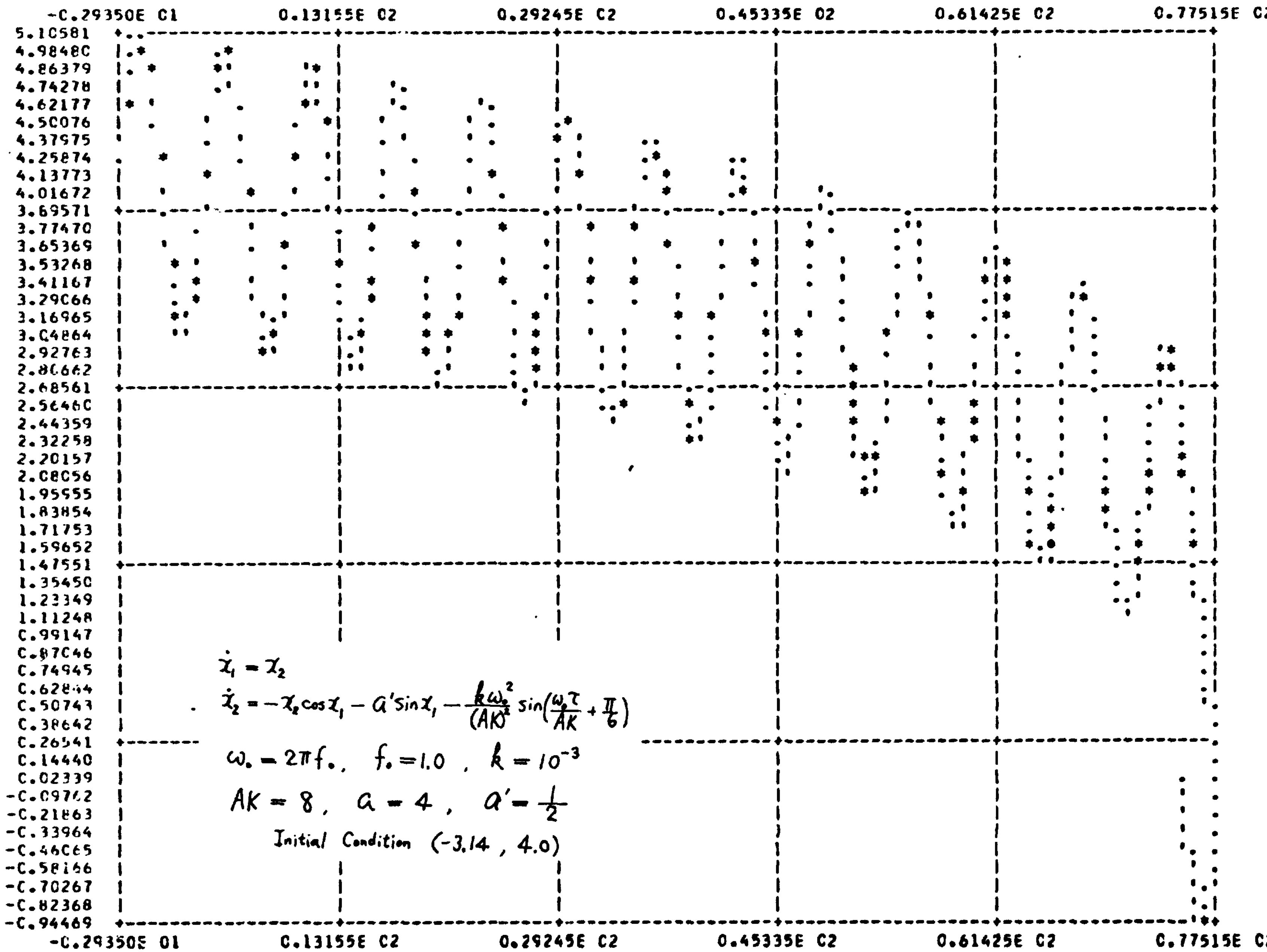

Fig. 11 (b)

S.M.U. SYSTEM SUBROUTINE - PLOTIT

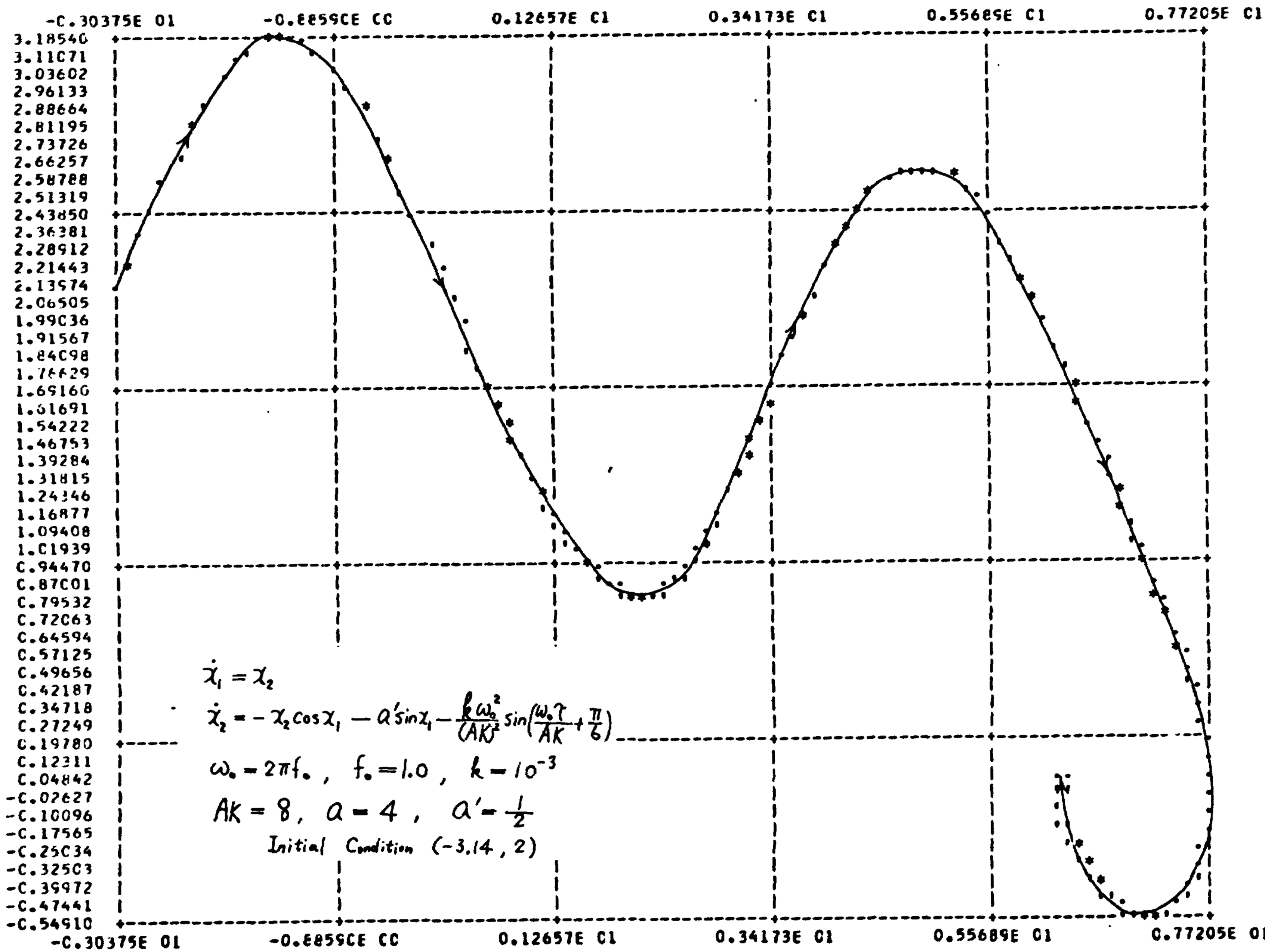

Fig. 11 (c)

S.M.U. SYSTEM SUBROUTINE - PLCTIT

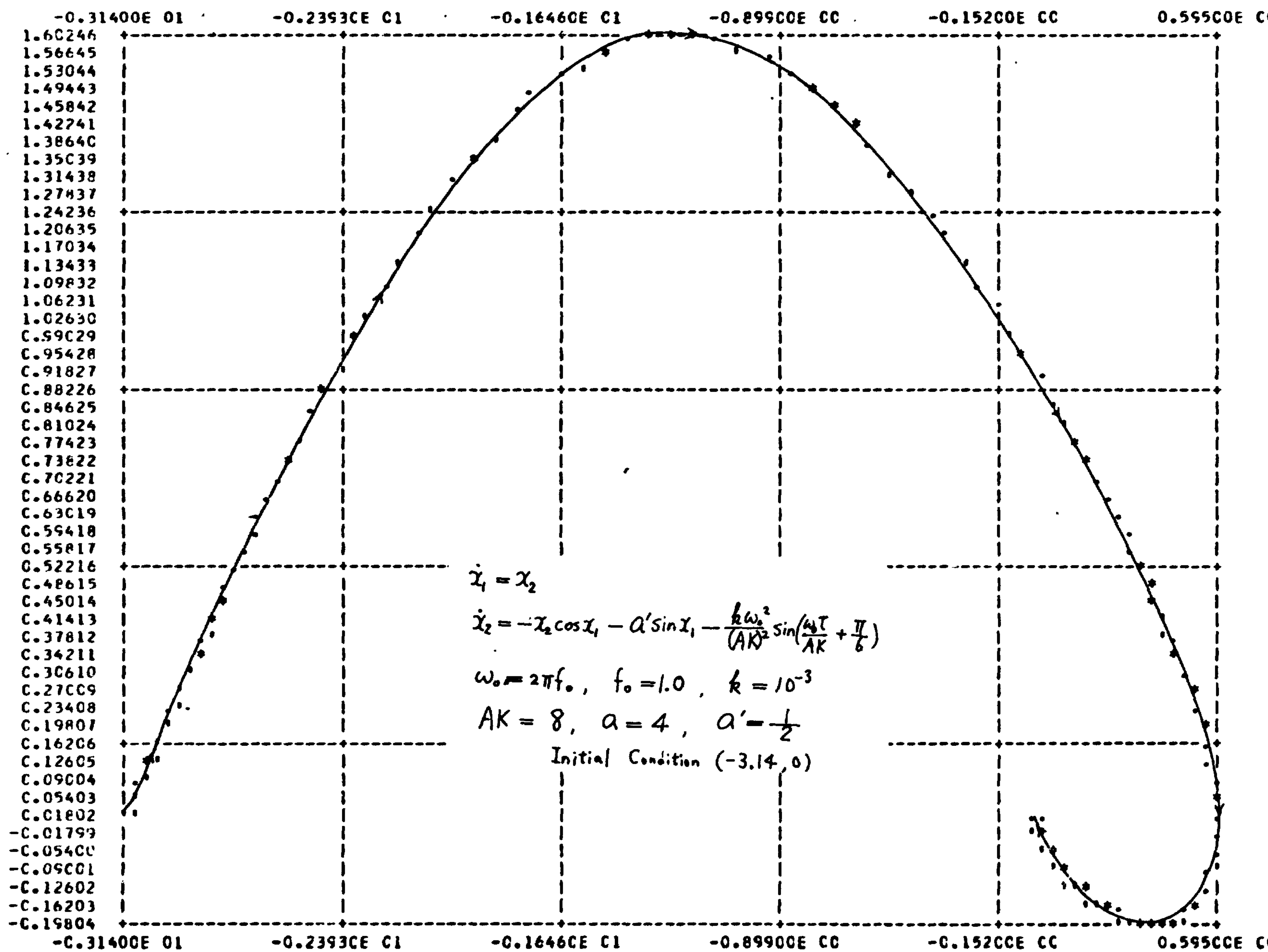

Fig. 11(d)

S.M.U. SYSTEM SUBROUTINE - PLCTIT

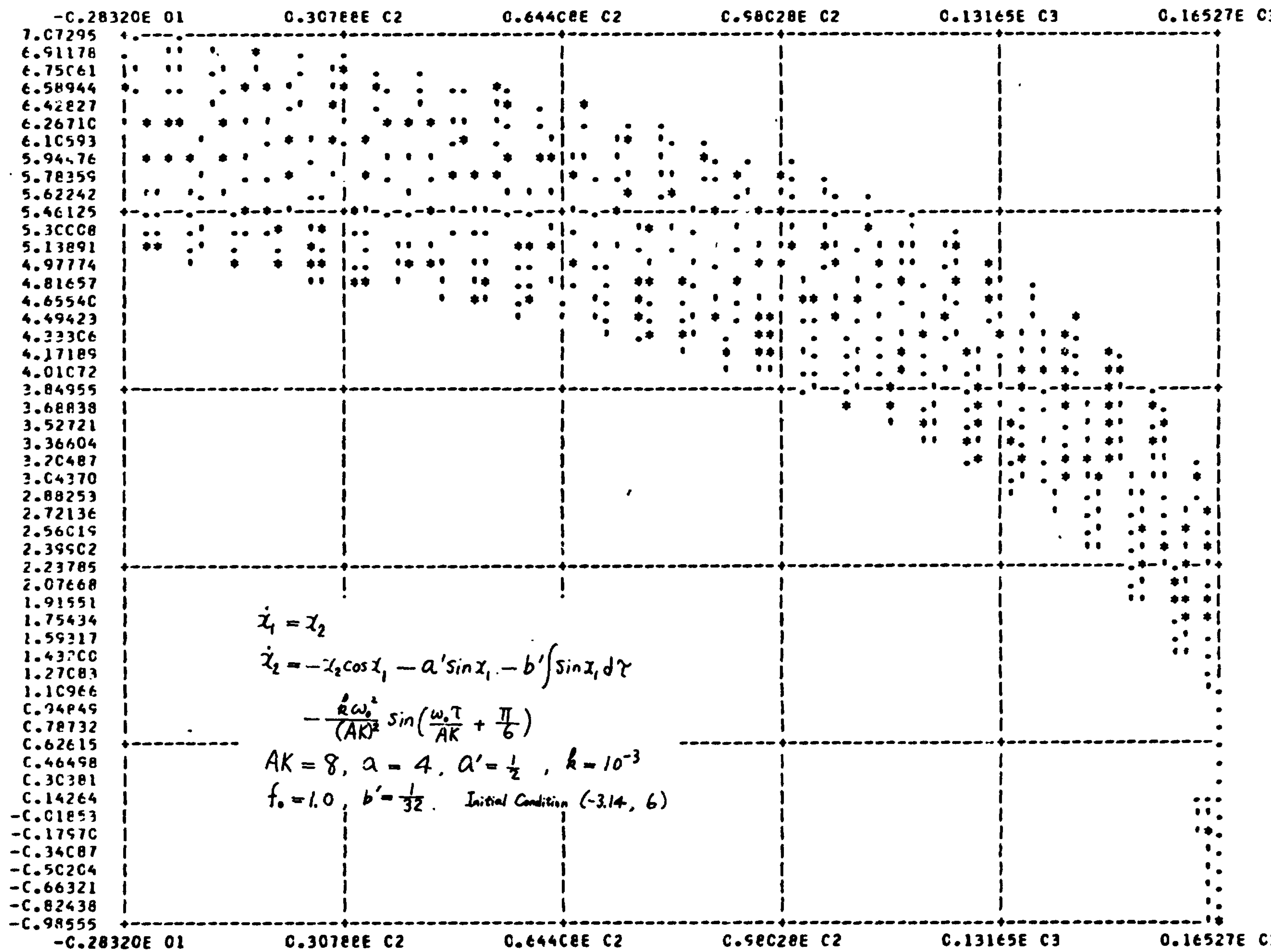

Fig. 12(a)

S.P.U. SYSTEM SUBROUTINE - PLCTIT

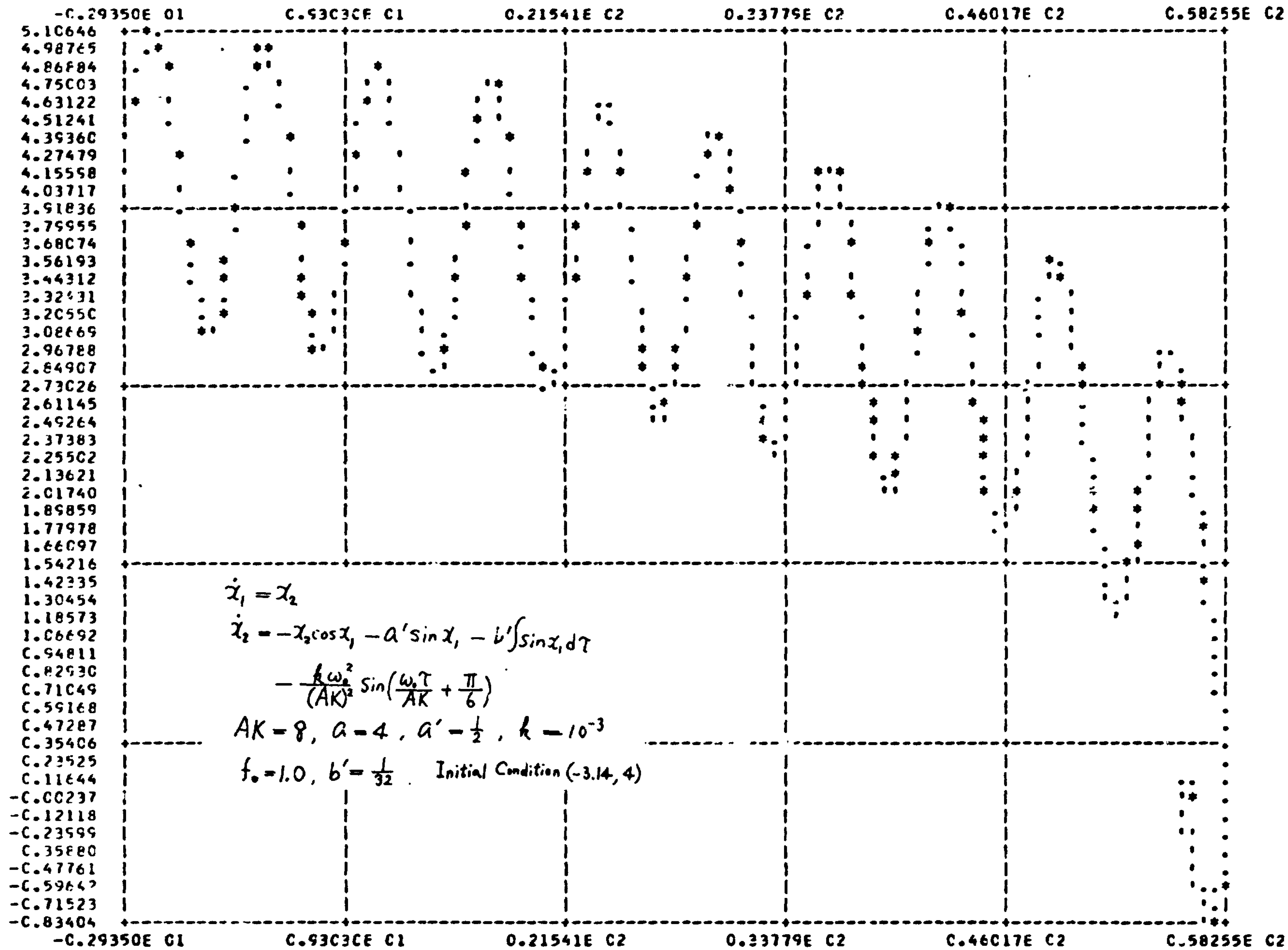

Fig. 12 (b)

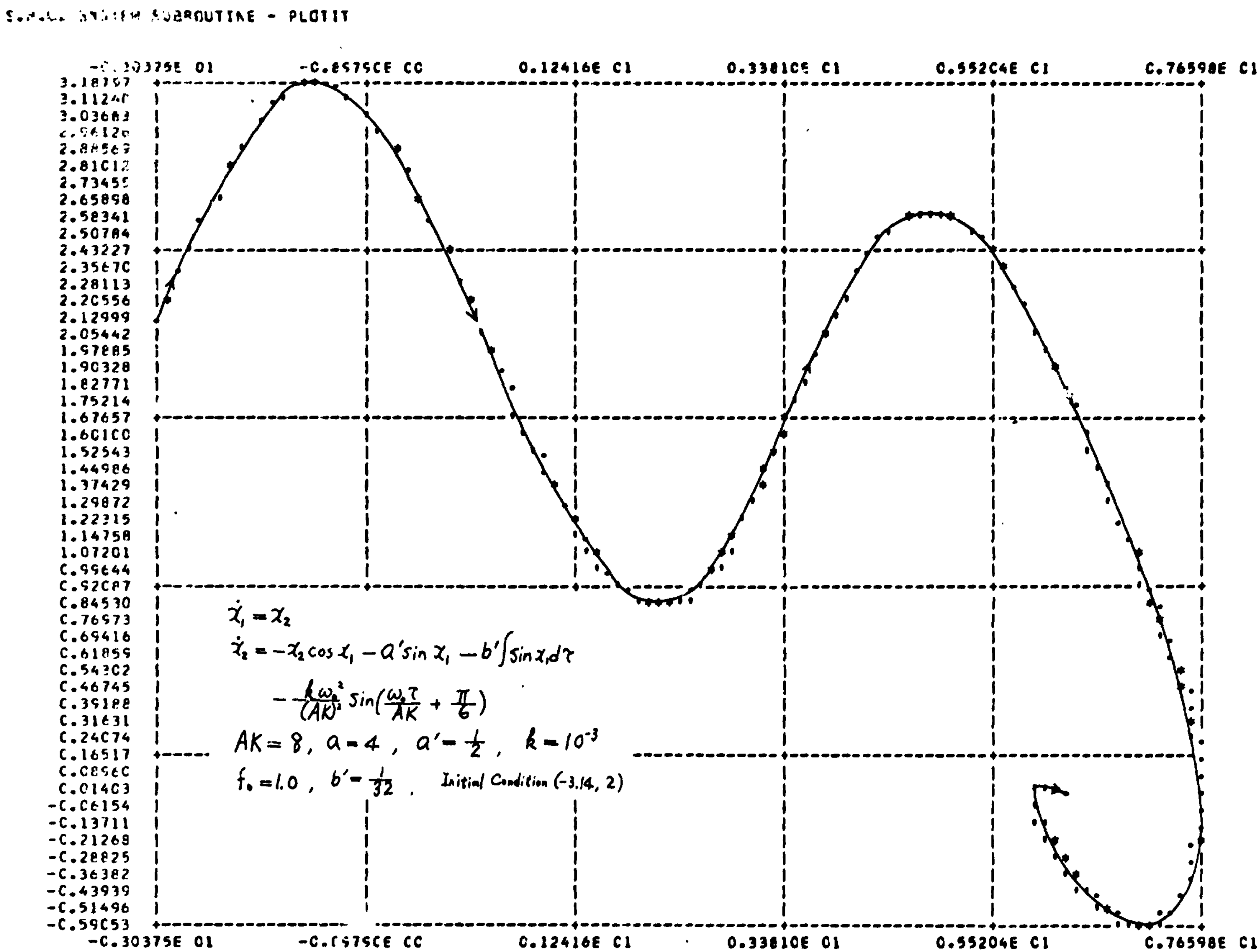
SUBROUTINE - PLOTIT
-C.30375E 01
-C.8575CE CC
0.12416E C1
0.33810E 01
0.55204E C1
C.76598E C1
2.43227
1.67657
C.92C87
C.16517
-C.59C53
$\dot{x}_1 = x_2$
$\dot{x}_2 = -x_2 \cos x_1 - a' \sin x_1 - b' \int \sin x_1 d\tau$
$- \frac{k\omega_0^2}{(AK)^2} \sin\left(\frac{\omega_0 \tau}{AK} + \frac{\pi}{6}\right)$
$AK = 8,\ a = 4,\ a' = \frac{1}{2},\ k = 10^{-3}$
$f_0 = 1.0,\ b' = \frac{1}{32}$, Initial Condition (-3.14, 2)

Fig. 12 (c)

S.M.L. SYSTEM SUBROUTINE - PLOTIT

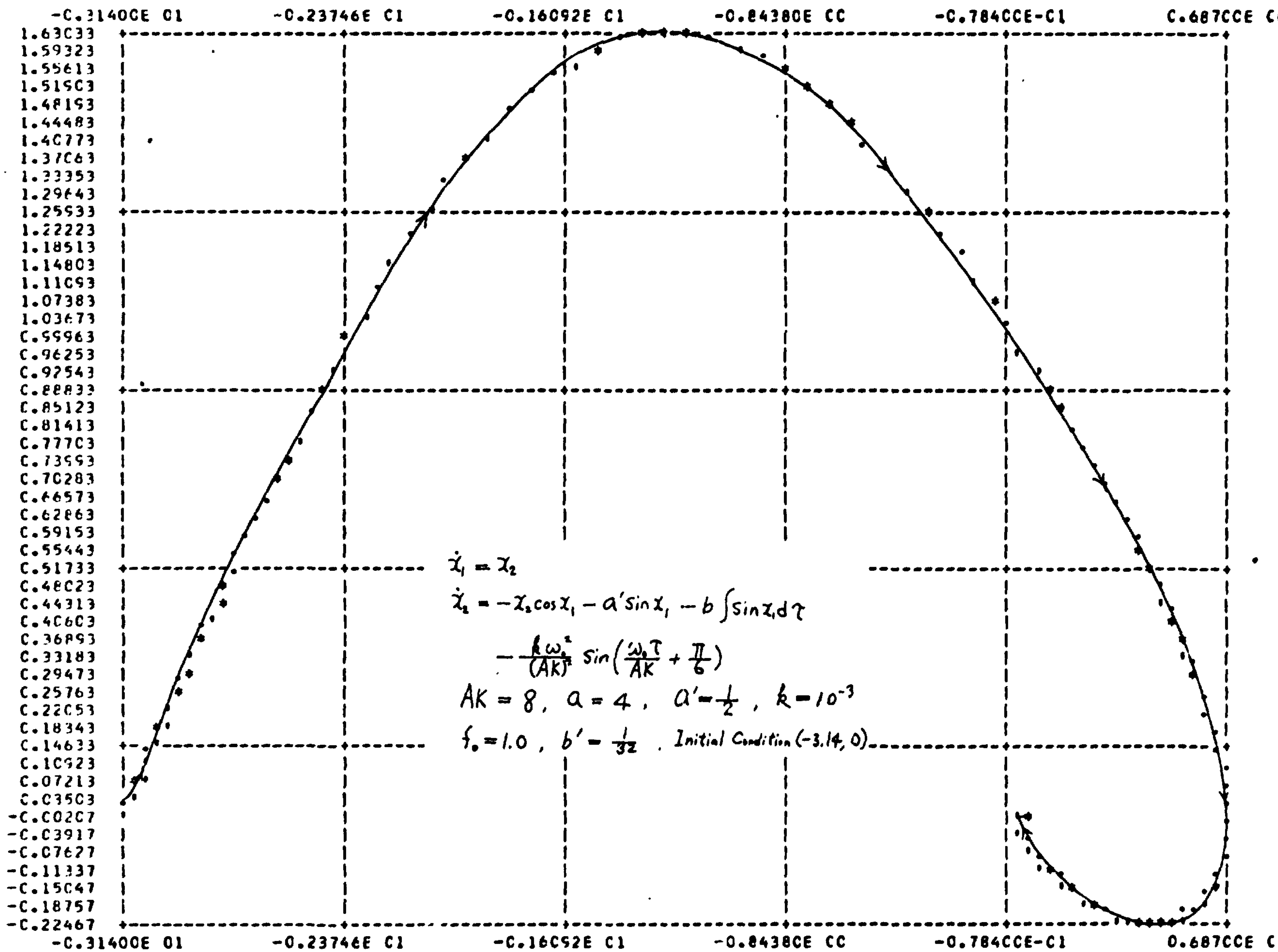

Fig.12(d)